Dynamics of Transport, Accumulation, and Export of Plastics at Oceanic Fronts

G. Suaria, M. Berta, A. Griffa, A. Molcard, T. M. Özgökmen, E. Zambianchi, and S. Aliani

Contents

Abstract Every year, vast quantities of plastic debris arrive at the ocean surface. Nevertheless, our understanding of plastic movements is largely incomplete and many of the processes involved with the horizontal and vertical displacement of

G. Suaria (✉), M. Berta, A. Griffa, and S. Aliani
Institute of Marine Sciences (ISMAR), National Research Council (CNR), Lerici, Italy
e-mail: giuseppe.suaria@sp.ismar.cnr.it

A. Molcard
MIO, Université de Toulon, Aix-Marseille Univ., CNRS, IRD, Toulon, France

T. M. Özgökmen
Rosenstiel School of Marine and Atmospheric Science, University of Miami, Coral Gables, FL, USA

E. Zambianchi
Parthenope University and CoNISMa, Naples, Italy

plastics in the ocean are still basically unknown. In this chapter we review the dynamics associated with the transport of plastics and other pollutants at oceanic fronts. Fronts had been historically defined as simple barriers to exchange, but here we show that the role of these structures in influencing the transport of plastics is more complex. The tools used to investigate the occurrence of frontal structures at various spatial scales are reviewed in detail, with a particular focus on their potential applications to the study of plastic pollution. Three selected case studies are presented to better describe the role of fronts in favoring or preventing plastic exchanges: the large-scale Antarctic Circumpolar Current, a Mediterranean meso-scale front, and the submesoscale fronts in the Gulf of Mexico. Lastly, some aspects related to the vertical subduction of plastic particles at oceanic fronts are discussed as one of the most promising frontiers for future research. The accumulation of floating debris at the sea surface is mainly affected by the horizontal components of frontal dynamics. At the same time, vertical components can be relevant for the export of neutrally buoyant particles from the surface into the deep sea. Based on these evidences, we propose that submesoscale processes can provide a fast and efficient route of plastic transport within the mixed layer, while mesoscale instabilities and associated vertical velocities might be the dominant mechanism to penetrate the deeper ocean on slower but broader scales. We conclude that given the ubiquitous presence of fronts in the world's ocean, their contribution to the global plastic cycle is probably not negligible and the role of these processes in vertically displacing neutrally buoyant microplastics should be investigated in more detail.

1   Introduction

Since plastic production began, humankind comprehensively produced around 8,300 million tons (Mt) of synthetic polymers [1], and every year, about 200 Mt. of municipal plastic waste are generated and disposed of around the world [2]. Of this amount, between 4.8 and 12.7 Mt of mismanaged plastic items are estimated to enter the oceans every year through various sources [3], an estimate which is predicted to grow up to 53 Mt per year by 2030, if significant global reduction measures for environmental plastic emissions will not be implemented [4]. As a result, plastic has been accumulating in marine ecosystems for decades, and synthetic polymers of various sizes, shapes, and typologies are now widespread, from the highly urbanized Mediterranean Sea to the most remote polar waters, although in varying concentrations [5–7].

Much progress has been made since the first reports of plastic pollution appeared in the scientific literature, and we now have a much better understanding of what are the main sources and impacts of many synthetic polymers commonly found in the

marine environment [5, 8]. However, a clear understanding of the global plastic cycle is still far from being achieved. According to the most recent global estimates, the total amount of plastic floating at sea (<0.3 Mt, [9–11]) represents only a small portion of the total estimated inputs in the marine environment (~8 Mt year^{-1}, [3]), although this theory has been recently challenged [12]. Recent studies suggested that backshores and coastal margins [13, 14], the water column [15, 16], or deep-sea sediments [17, 18] can all be accounting for this missing fraction [19]. In spite of this growing body of information, this remarkable mismatch demonstrates that our understanding of plastic fluxes and pathways between different compartments is largely incomplete, and some fundamental aspects of plastic transport and distribution in the ocean are still basically unknown.

Plastic concentration is very inhomogeneous in the ocean. Research has shown that high-concentration zones occur not only at the large scale in oceanic garbage patches, but they are distributed in all regions at various spatial scales and intermittent in time [20]. This inhomogeneity can lead to an important sampling bias, with obvious consequences for global plastic estimates. At the same time ocean plastics occur in a wide range of size classes, further complicating our understanding of the main factors associated with their cycling through the marine environment. A comprehensive description of the main physical processes driving and influencing horizontal and vertical debris transport at different scales of ocean dynamics has been recently made by van Sebille et al. [21]. The large-scale dynamics responsible for the well-known "garbage patches," i.e., the floating litter accumulation zones found at midlatitude in all the world's oceans, has been studied by many authors (e.g., [9, 10, 22]; other references in [21]), but in general, scant information is available about the small-scale transport of debris driven by submesoscale, 3D turbulence, and microscale processes. The transport of other pollutants by mesoscale eddies, geostrophic currents, and internal waves is better reported [23–27]. At the same time, the continuous findings of massive debris accumulations on the seafloor (including low-density polymers) suggest that one of the ultimate sinks for plastic debris is the deep ocean, and that marine sediments can be likely considered as a final plastic repository [28–30], although the role of resuspension mechanisms, especially in the presence of intense benthic nepheloid dynamics still needs to be clarified (c.f. [31]). In the upper ocean, therefore, there must be processes capable of removing plastic from the sea surface and transporting it to the deep sea.

In principle, once in the marine environment, plastic particles (here defined as synthetic particles smaller than a few millimeters), as any other small particles in the ocean, move together with the surrounding water, and with a good approximation the movement of plastic particles follows the movement of water parcels [21]. In an ideal uniform flow, the relative distances of particles in the flow, i.e. its dilution or accumulation, would mainly depend on the particle's properties (e.g., size, buoyancy, density) rather than on the fluid's properties. But in the actual ocean, the flow is highly complex and the physical properties of ocean currents play a very important role in shaping and defining plastic distribution. In addition, many plastic items such as expanded polystyrene and synthetic foams also contain trapped air, which further increases their buoyancy, subsequently aiding their wind-mediated dispersal. So, if

we want to understand plastic movements in the oceans, we first need to understand ocean dynamics and their spatio-temporal variability. From this point of view, a better understanding of the physical processes governing the transport of solid pollutants in the marine environment is a fundamental prerequisite to finally close the plastic budget, ultimately improving our capacity to address and mitigate the negative impacts of this global emerging challenge.

Oceanic fronts are physical features that have not been investigated thoroughly with respect to plastic litter. These frontal systems are often characterized by the presence of convergence zones that accumulate floating debris at the ocean surface together with planktonic organisms and higher trophic levels organisms attracted by enhanced productivity [32, 33], and downwelling areas that can potentially export neutrally buoyant debris into the deep sea over short distances possibly contributing to their final sinking. Convergences at frontal zones have the potential to boost the interactions between litter and marine life, when high densities of plastics and frontal processes coexist. Ingestion, entanglement or colonization of litter surfaces increases [32] with many consequences. The ingestion likelihood of plastics depends on the probability for the species to encounter debris, therefore planktonic organisms passively accumulated in the convergence zones are more susceptible to plastic ingestion, but at the same time, also ocean-going predators can be attracted by an increase in local preys' abundance and by the shade created by large floating debris that attract both small fish and large predators around them [34]. Interactions of biota with plastics at frontal convergence zones are also relevant as the growth of biofouling can noticeably alter the buoyancy of the plastic particles [35–37], thus favoring and/or accelerating their sinking velocities [29, 38]. Nevertheless, the available literature on these processes is still very limited, even at the ocean surface, where sampling tends to be easier. The ubiquitous presence of fronts in the world's ocean at any spatial scale suggests that the global contribution of these structures to the plastic cycle is probably not negligible and the roles of these processes in creating surface concentration zones and in removing debris from the sea surface are not fully understood yet.

In this chapter we focus on the transport, accumulation, and export dynamics of plastic debris and other pollutants at oceanic fronts (Sects. 2 and 3). The tools used to investigate the occurrence of frontal structures at various spatial scales are reviewed in detail, with a particular focus on their potential applications to the study of plastic pollution (Sect. 4). Three selected case studies are presented to better describe the role of fronts in favoring or preventing plastic exchanges: the large-scale Antarctic Circumpolar Current (Sect. 5.1), a Mediterranean mesoscale front (Sect. 5.2), and the submesoscale fronts in the Gulf of Mexico (Sect. 5.3). Lastly, some innovative aspects related to the vertical subduction of plastic particles at oceanic fronts are presented as one of the most promising frontiers for future research (Sect. 6).

2 Fronts as Boundaries for Plastic Exchanges

Fronts are defined from the geometrical point of view as areas characterized by a strong gradient in one direction (cross-front), and a much weaker gradient in the perpendicular direction (along front). They can be characterized by various physical and biogeochemical properties and are commonly observed at the ocean surface with scales that can vary from kilometers to meters. The process of frontal formation and sharpening is called frontogenesis [39] and is especially prominent and fast acting in the case of active fronts based on density gradients, involving the development of vertical secondary circulation in the cross-front direction [40]. The frontogenetic processes lead to enhanced gradients of physical properties such as temperature and salinity, that determine density, but also of the chemical and biological properties that characterize the water masses. Indeed, it is often observed that fronts are not typical of just one property but are usually reflected in many properties [41, 42], with separation sometimes clearly visible by macroscopic water properties e.g., color, particle loads, foams, and flotsams including anthropogenic litter (Fig. 1). While fronts appear mostly as horizontal boundaries, various instability processes occur at different scales that can facilitate property mixing. They include mesoscale instabilities, generating meanders and eddies, and submesoscale instabilities, generating smaller features and active convective cells. So, the interaction between water masses involves a set of complex dynamics at different spatial scales and not a simple separation.

Oceanic fronts occur on a variety of scales, from a few meters up to many thousand kilometers [39]. Some of them are short-lived, but most of the large- and mesoscale fronts are quasi-stationary and seasonally persistent: they emerge and disappear at the same locations during the same season, year after year. The most prominent fronts are present year-around. Small submesoscale fronts, on the other hand, associated with mixed layer inhomogeneities or water mass filaments detaching from mesoscale eddies or jets typically have very short time scales, of the order of days, and lead to mixed layer restratification. There is no definitive classification of fronts, but a partial listing of them would include tidal fronts, upwelling fronts, estuarine fronts, shelf-break fronts, river plume fronts, fronts associated with the convergence or divergence of water masses in the open ocean, frontal eddies, and fronts associated with geomorphologic features such as headlands, islands, and canyons [43]. All of them have the potential to concentrate flotsams and contaminants, although with different effectiveness, but so far, the actual presence of debris at frontal systems has not been studied as deeply as other pollutants [44, 45].

Alternating zones of downwelling and upwelling flow are usually produced in correspondence of frontal systems. These phenomena can induce vertical flows enhancing, in turn, peculiar physical and biological features. Converging surface water necessarily sinks at the front line [46], separating light and heavy waters that form a floating lens of light water around the convergence and a downwelling plume of dense water, respectively. Zones of convergence are a common pattern in oceanic

Fig. 1 Airborne images of surface frontal systems: in the top panel oil slicks aligned into a front in the Gulf of Mexico. In the bottom panels: fronts associated with the Mississippi river input into the Gulf of Mexico. The water masses have different optical properties that can be spotted in the visible field from airborne images (Photo credit: Maristella Berta)

fronts. Similar to water parcels, debris is transported toward the convergence where the heavy portion sinks and lighter floating material (natural or anthropogenic) accumulates at the surface where it is visible by naked eye and at least in theory, by satellites too [47–50]. Preliminary data and modeling experiments suggest that in frontal convergences, surface accumulation processes can generate densities of floating litter (and other pollutants) orders of magnitude higher than in the surrounding waters [51–55], but dedicated experiments are necessary for an accurate description and quantification of these structures' concentration properties.

Even though fronts can form at any depth, it should be emphasized that in the following sections we will mainly focus on surface fronts for the purpose of studying their interactions with marine litter. Although some data on the vertical distribution of microplastics along the water column are starting to appear in the scientific literature (see Liu et al. [56] for a recent review), virtually no data exist about microplastics in the water column at deep oceanic frontal systems. As a matter of fact, the vertical distribution of floating plastic depends not only on the particle's buoyancy, but also on the dynamical environment induced by vertical movements of ocean water (see Sect. 6). So, downwelling at frontal systems has the potential to sequester floating material from the ocean's surface and can be considered as potential debris sinking zones from the surface to the ocean interior [21]. The transport of material at the ocean surface, however, is expected to play a major role for most buoyant and nearly buoyant plastics (i.e., the majority of all synthetic polymers currently produced worldwide). In addition, surface fronts are indeed the most active ones from the physical point of view, not only because of the direct interaction with atmospheric forcing, but mostly because the absence of vertical velocities at the interface between ocean and atmosphere allows for enhanced stirring within mesoscale eddies, causing gradient sharpening and therefore further enhancing frontal properties [40, 57, 58].

3 Ocean Currents and the Transport of Plastics: A Problem of Scale

Focusing on surface processes, over the past few decades, there has been a tremendous amount of progress in understanding and predicting ocean currents and their associated transport of anthropogenic pollutants. Perhaps a suitable beginning for such rapid progress can be attributed to MODE, i.e. the Mid-Ocean Dynamics Experiment [59] during which "ocean weather" consisting of mesoscale eddies on spatial scales of hundreds of kilometers, evolving on time scales of months was discovered. This view of the ocean containing long-lasting coherent structures is different from the earlier perspective based on a large-scale mean flow that governs the advection of material for years and decades. Early numerical modeling using quasi-geostrophic equations (arising from a balance of forces between the Earth's rotation and pressure gradient) showed that barotropic and baroclinic instabilities lead to a ubiquitous emergence of mesoscale eddies in the ocean circulation [60].

The second major step forward was taken with the advent of satellite oceanography, in particular the Topex/Poseidon mission, which allowed estimation of sea surface height anomaly over the range of scales from 100 km to several thousand kilometers [61]. Using the geostrophic approximation, only a few satellite altimeters allowed estimation of much of the ocean's near-surface velocity field uninterrupted by cloud coverage [62]. The availability of horizontal velocity data from satellite measurements allowed calculation of many quantities of interest. One such quantity

is the turbulent kinetic energy spectrum. This is important not only for parameterizing and modeling turbulence, but also for improving the accuracy of climate forecasts.

The zeroth-order expectation, on the basis of high aspect ratio (lateral vs vertical scale) and strong influence of rotation, would be that the ocean exhibits 2-dimensional (2D) turbulence characteristics at geostrophic scales, with the wavenumber power spectrum of kinetic energy obeying a power law. However, estimates based on satellite altimeter measurements consistently showed a slope that is flatter than expected [63]. This result indicates that the ocean's surface is more energetic than can be explained on the basis of 2D turbulence alone. The mechanism causing this discrepancy in slope was not immediately clear, until the realization of the relevance of the so-called submesoscale flows. The existence of small-scale convergent circulations in the ocean was known long before [64]. More recently, it has been demonstrated that the slope can be also altered by barotropic tides and their interaction with mesoscale dynamics [65, 66]. Submesoscale dynamics, however, are currently surmised to act as a main conduit between the nearly-2D geostrophic mesoscales and classical 3D turbulence [67, 68].

Submesoscales are generically defined as flows on the margin of loss of geostrophic balance, with Rossby number (i.e., ratio of relative and planetary vorticity) on the $O(1)$, with horizontal space scales of 0.1–10 km and evolution time scales of hours to days. Visible observations from the Space Shuttle of spiral eddies with radii of 5 km [69] and satellite observations of chlorophyll supported the notion that such flows exist in the ocean. The reader is referred to reviews by McWilliams [70] and Klein et al. [71] for full references on submesoscale flows. For the purposes of this chapter, it is important to note that the first order effect of submesoscale flows is a change in the character of the flow from being mostly rotational to mostly convergent at the surface. As such, submesoscale flows are intimately related to the transport of all surface material [72].

Overall, then the emerging picture of transport in the ocean points toward a complex time integrated function of processes ranging from large scales (>100 km and order 1 month), to mesoscales (in the range 100–10 km and month-days), reaching submesoscales (in the range 10–0.1 km and 1 day), and high frequency processes such as waves and 3D turbulence. All these scales and processes interact and, as we will see below, their relative importance depends on the specific problem and application considered.

4 Tools, Prediction, and Validation Methodologies

Several tools are currently available to study and improve our knowledge about the processes discussed above. Indeed, the occurrence of floating macro and microplastics in the marine environment has been traditionally studied by net sampling (for microplastics) and visual surveys (for macroplastics). A detailed description of the methods used for sampling and measuring ocean plastics is out

of the scope of this chapter, but comprehensive reviews can be found in Hidalgo-Ruz et al. [73] and Mai et al. [74], among the others. For the purposes of this section, it is important to keep in mind that these techniques have important limitations, as discrete, point samples are often too sparse in space and time to provide enough coverage for accurately describing dynamic events such as accumulation and/or dispersal of plastics at oceanic fronts. In addition, ship-based visual transects and/or surface net trawls often integrate information over scales of a few kilometers or hundreds of meters, which are too coarse to accurately describe accumulation dynamics happening at much smaller spatial scales. Therefore, due to the inadequacy of the most commonly used sampling methods and to the previously mentioned high spatial heterogeneity in plastic distribution over the ocean surface [20], traditional sampling tools should always be integrated with other observational methods that help locate the sampling results within the current velocity field, in order to fully understand the effects of physical processes on plastic transport and accumulation dynamics.

It is worth mentioning that the majority of techniques described in this section – such as HF radar, Lagrangian drifters, satellite and airborne data – are intrinsically devoted to the study of the ocean surface, as this is where most of the work has been done so far. Surface measurements can provide useful synoptic information and are very valuable for identifying the surface expression of oceanographic fronts at various spatial and temporal scales. This is often the first, important step, to guide more in-depth observations at fronts, using research vessels or gliders [75].

From the ocean dynamics point of view it is well known that water column dynamics plays a key role in changing ocean stratification and the mixed layer structure through vertical fluxes of mass, energy, and tracers [58, 76]. Indeed, surface information alone is not able to fully resolve the complex 3D pathways that are expected to influence plastic movements in the ocean. Therefore, besides allowing to characterize surface transport in greater detail, the joint use of surface measurements and 3D numerical models is very promising in investigating and improving the accuracy of plastic transport pathways predictions at sea and for this reason 3D ocean dynamics represents a very active field of research which is already showing promising results [75, 77–79]. At the same time there is mounting evidence about the increasing presence of submerged plastic debris, either on the seafloor [17, 28, 80] and in the water column [15, 81], even though subsurface transport processes and plastic sinking behavior are still far from being thoroughly understood. Vertical dynamics plays also a major role in oil spill events where multiple phases fluxes (liquid, gas, and heat components) interact with ocean turbulence and mixing processes [82–84]. So, as we further suggest in Sect. 6, direct measurements of both the physical ocean dynamics and the tracer's component remain critical for a comprehensive understanding of 3D current structure and its role in the fate and vertical displacement of oil, plastic debris, and other contaminants [21, 85].

4.1 Lagrangian Drifters

Transport properties of oceanic and coastal flows have been widely investigated both at the regional scale and at global level through the deployment of drifters since the 1980s. Modern drifters are floating devices equipped with Global Navigation Satellite Systems (GNSS) receivers designed to drift with currents at different depths according to the shape and depth of the underwater drogue (Fig. 2). The most common and widespread types are the "Coastal Ocean Dynamics Experiment" (CODE) drifter [86] sampling the first meter of water, and the "Surface Velocity Program" (SVP) drifter [87] sampling currents at 15 m depth. Some of these devices may also carry other sensors, for example measuring surface temperature, or atmospheric pressure, used for cross-validation of remote sensing observations and for monitoring climate variability [88]. In the last years, new designs of drifters have been proposed, and particular attention has been devoted to minimize the environmental impact of deploying expendable devices at sea. For instance, the surface (60 cm-depth) drifter developed by the Consortium for Advanced Research of Transport of Hydrocarbon in the Environment (CARTHE) is designed to be 85% biodegradable [89]. The CARTHE drifter has been widely used for massive deployments in the Gulf of Mexico to unravel surface transport pathways in areas deeply exploited by oil and gas companies, to describe the fate of oil released into the environment, and to inform and guide mitigation efforts [90].

GPS drifter-based connectivity studies allow the investigation of passive transport processes through the analysis of drifters' trajectories. These studies find application in many scientific fields, since ocean currents have a crucial role in mixing ocean properties as well as in carrying and dispersing floating material and substances of anthropogenic and natural origin [91]. The investigation of predominant transport pathways driven by currents through drifters, together with modeling
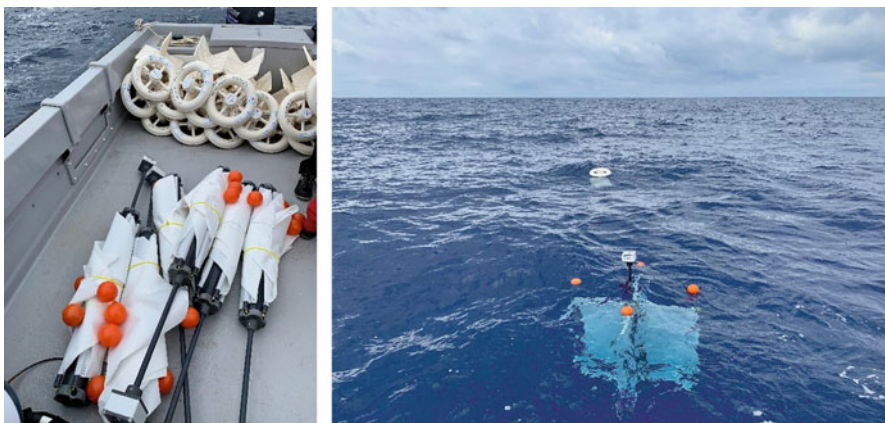

Fig. 2 CARTHE (top) and CODE (bottom) drifters before (left panel) and after (right panel) deployment at sea (Photo credit: Maristella Berta)

and genetic studies [92–95], puts in evidence the connectivity among neighboring sea areas, that is used to study sources and fate of biological material influencing population distribution and dynamics [96]. These studies introduce the important concept of oceanographic distance, for which two sea areas may be geographically next to each other but their exchange of properties and substances is enhanced (or inhibited) by the currents encompassing them [97]. Therefore, a specific area may preferentially exchange water properties with an area not necessarily spatially adjacent, because prevailing sea currents put them in connection [98].

The importance of oceanographic connectivity among remote areas, and of the time scales involved, has been evidenced as well in studies investigating the complex pathways of floating marine debris both at global and basin scales. For example, Maximenko et al. [99] analyzed global drifter trajectories to identify five major oceanic debris accumulation areas centered in the subtropical gyres; van Sebille et al. [100] investigated the origin and evolution of the global garbage patches from observational data of the Global Drifter Program in the open ocean and coastal regions on interannual to centennial timescales; and Zambianchi et al. [101] used the historical Lagrangian dataset collected in the Mediterranean Sea since the 1980s to estimate the probability of debris particles reaching different sub-basins.

The distribution of plastic debris and biological material is also strongly affected by processes taking place at the meso- and submesoscales, and in particular along fronts, where the interaction of different water masses drives the transport and accumulation of substances. For instance, in the framework of the 2016 CARTHE experiment in the Gulf of Mexico, devoted to the investigation of oil spills' dispersion properties, D'Asaro et al. [102] characterized the effectiveness of submesoscale frontal activity to organize surface material by analyzing surface drifter trajectories launched across a frontal zone and converging along the frontal line. Customized surface drifters have also been used by Meyerjürgens et al. [103] to investigate marine litter pathways in the German Bight, characterized by high concentration of floating debris coming from the English Channel, and rich of submesoscale fronts in the coastal and estuarine area, shaping surface accumulation patterns of floating debris. Similarly, an interesting citizen science-based wooden drifter launch and recapture approach was used by Schöneich-Argent and Freund [104], to investigate the dispersal and accumulation of floating litter from coastal, riverine, and offshore sources in the German Bight.

The GPS drifter release campaigns provide valuable and direct information on surface transport trajectories. Dispersion properties can also be drawn from single or multiple particle statistics (Taylor [105] and Ottino [106], respectively; see the review by LaCasce [107], and the recent assessment of different dispersion regimes in the ocean from drifter data by Corrado et al. [108]), but generally require a large number of drifters to be released. The analysis of the dispersion properties gives a picture of the regimes characterizing the circulation, and may help to evidence regions of marine debris accumulation or transport barriers. However, it is difficult and rare to repeat these campaigns with real drifters or to make massive releases such as those performed by the CARTHE experiments. Most observational experiments generally use $\sim O(10)$ drifters, whereas virtual particle-tracking experiments can

release $\sim O(10000)$ or more particles, thus overcoming this limitation. Since numerical models and HF radars provide Eulerian fields, larger statistics could be easily obtained on synthetic Lagrangian trajectories based on the velocity field for advection, plus, in case, a parameterization of subgrid-scale, diffusive processes.

4.2 Eulerian Velocity Fields

As a first approximation plastic particles could be considered as passively advected water parcels. Therefore, knowledge of surface currents is essential to study the distribution of plastics at the ocean surface. There are currently only two ways to obtain temporal evolution of total (geostrophic and ageostrophic components) synoptic surface currents over large horizontal areas: numerical models and HF radars, or a combination of both via data assimilation techniques. Satellite remote sensing currently only provides fairly coarse information on sea level from which only the geostrophic component can be deduced.

Numerical models applied to the ocean are now acknowledged for their validity and performance thanks to the increasing data assimilation and computer capabilities. The Navier-Stokes equations, more or less approximated (hydrostatic, Boussinesq, LES) are discretized and numerically resolved on a mesh, which defines the spatial resolution. Subgrid-scale processes are parametrized with empirical formulae based on theoretical, in-situ and laboratory experiments. While being aware of the limitations of the numerical approach, it is still the only way to have a three-dimensional, synoptic view of hydrology and ocean dynamics, and to make realistic forecasts [109]. The age of machine learning and artificial intelligence may change this principle in the coming years. Most of the research that has been done in the last decade on marine debris was based on these numerical simulations, to predict, and later confirm the existence of the great Pacific garbage patch or other large-scale convergence zones, as well as to highlight the main driving forces behind large-scale plastic distribution patterns (e.g., Lebreton et al. [110]; Maximenko et al. [99], and many others). More recently, higher-resolution numerical models have been also applied to study the dynamics of litter movements at oceanic fronts and at smaller spatial scales [26, 52].

On the observational side, HF radars can produce coastal surface current maps at high spatial and temporal resolution over a relatively wide range (up to 200–250 km). They are land-based remote sensing instruments that gained popularity in the last few decades [111–113]. Their functioning is based on the coherent Bragg scattering from the "lattice" represented by surface gravity wave trains propagating at the surface of coastal basins. This happens when their typical wavelength approaches half the wavelength of the electromagnetic radiation emitted by the radar. A first Doppler shift in the frequency of the backscattered signal occurs if surface waves approach or recede from the transmitting antennas. A second Doppler effect is associated with the presence of currents underlying the gravity waves, from which it is possible to compute the surface velocity field. Since this

procedure provides the radial current with respect to the antenna location, it is necessary to have at least two stations to reconstruct the surface velocity vector field. HF radars are characterized by very high spatial and temporal resolution; the former is determined by the operating frequency of the radar, which in turn dictates its range and coverage (see Table I in Rubio et al. [113]). Their characteristics allow to get a repeated in time, synoptic view of surface currents which would be otherwise unobtainable from in-situ or space-based remote sensing techniques. More recently, also ship-based X-band marine radars emerged as useful tools for diagnosing frontal features in offshore areas [114] as well as floating patches of plastic debris in coastal areas [115].

It is clear from above that such systems, as well as the numerical models, do not provide direct measurements of plastics or other pollutants floating at the ocean surface. However, synoptic observations of the surface current fields can be used to reconstruct the transport and fate of buoyant substances, which can then be validated or ground-truthed by field sampling. This is best done through Lagrangian, i.e., water following methods, as discussed in the following sections. However, in the framework of fronts' identification, the approach of using high-resolution numerical models is very powerful, as dynamical velocity-based fronts can be associated with strong gradients in the water mass characteristics. The time evolution of the 3D front shape can be followed [116, 117], as well as the interactions with the atmosphere (wind-stress, air-sea fluxes) and the surrounding environment (gyres, coast, etc.). The required resolution necessary to simulate surface fronts is the mesoscale to submesoscale (depending on the Rossby Radius of deformation). Eventually, the non-hydrostatic versions of a numerical model may improve the resolution of the strong vertical velocities associated with fronts. HF radars could evidence sharp velocity, vorticity, and divergence gradients that may reflect the presence of a coastal front often associated with a boundary current system. By associating information about surface currents obtained with HF radars and numerical models with particle advection, one can obtain a good representation of plastic distribution and accumulation pathways.

4.3   Virtual Trajectories and Lagrangian Coherent Structures

The Eulerian velocity fields described in Sect. 4.2 can be used as a basis to compute virtual particle trajectories, i.e., to provide the so-called Lagrangian view of the flow. The Lagrangian description is especially useful to describe transport, and many Lagrangian metrics and tools have been used to provide indications on passive transport of pollutants such as plastics. Many of the historical metrics used to describe passive particle behavior are based on the concepts of dispersion. Single particle or absolute dispersion describes the average distance covered by a random particle from its initial condition over a given time, while two-particle dispersion provides the average distance between particle pairs [105, 106]. These statistics characterize the main spreading properties of a passive tracer and can be used also to

characterize different fluid dynamic regimes (see, for instance, reviews by Corrado et al. [108] and LaCasce [107]). Dispersion properties have been computed in the ocean using in-situ GPS drifters (see Sect. 4.1) but their number is always necessarily limited. For this reason, using virtual particle in numerical models is considered a very useful approach to complement and guide direct in-situ observations.

Different Lagrangian particle-tracking models coupled to ocean circulation models have been widely used to evaluate and predict distribution and beaching of marine debris, assuming a 2D approach. Neglecting the complex 3D physics or the biological processes experienced by different plastic items during their journey does not preclude interesting results. At the global oceanic scale, Lebreton et al. [110] simulated 30 years of plastic debris distribution with specific continuous input (rivers or cities) resulting in accumulation zones in the large oceanic gyres. Martinez et al. [118] or Lebreton et al. [22] included additional transport mechanisms (Stokes drift and windage) and analyzed long-term marine debris pathways. Equivalent studies have been carried out at basin and regional scales [26, 119–121], yielding interesting results on the main regional drivers and patterns of floating litter distribution.

Broadening the perspective to HF radar Lagrangian studies for the very purpose of pollutant transport studies, the stage for specific HF radar application to oil pollution events was set back in 1998: Heron et al. [122] looked at the spreading of a patch of Lagrangian particles advected by the surface current field observed by a HF radar in Port Phillip Bay, Australia. Uttieri et al. [123] studied the onset of a major pollution outbreak in the Gulf of Naples. Mantovanelli and Heron [124] used Lagrangian reconstructions obtained on the basis of HF radar-derived surface velocities in the Australian Great Barrier Reef area to investigate the fate of oil spilled by a coal carrier, as well as the spreading of estuarine and inshore waters probably responsible for the spreading of a fish disease. Transport studies, focused on oil spill applications, based on HF radar data were also performed in the framework of the TOSCA project [125], also using non-conventional blending techniques [126] of radar observations with other sources of information (drifters). More recently, Sciascia et al. [96] and Cianelli et al. [127] looked at biological transport in two coastal regions through forward and backward Lagrangian reconstructions, respectively; the latter paper, in particular, succeeded in discriminating between physical and biological mechanisms in species succession. While some work has been recently done using X-band radars [115], to the best of our knowledge, HF radars have not yet been used to study the movements and dynamics of plastic debris, and this will surely represent a future promising application for this useful technology.

An additional powerful tool that could help to easily identify accumulation or divergence areas in the velocity field that could impact plastic transport is the Lagrangian Coherent Structure (LCS) method, coming from the dynamical systems theory and recently applied to geophysical fluid dynamics [128–132]. LCS are lines or surfaces that can act as barriers between regions where tracers exhibit different behaviors, and can be easily mapped with the largest Finite-Time (FTLE) or Finite-Size (FSLE) Lyapunov Exponents. Where the FTLE measure the exponential rate of separation of trajectories initially close, FSLE measure the time required for particles

to separate. These methods require a large number of particles which motivates the use of virtual trajectories and have been recently used to characterize regimes of dispersion and mixing [133, 134], to effectively correlate LCS barriers with frontal regions [135], as well as to successfully identify sources, pathways, barriers and transport dynamics of anthropogenic debris in subtropical embayments [136, 137]. Other derived Lagrangian metrics (Finite Domain Lagrangian divergence or Lagrangian Eddy Kinetic Energy) have also been recently used to relate frontal dynamics and small-scale processes to phytoplankton distribution [138, 139].

4.4 Remote Sensing

Since the launch of TOPEX/Poseidon and ERS-1 missions in the early 1990s, the growing constellation of altimetric satellites observations allowed us to characterize large-scale ocean circulation variability down to mesoscales [140–142]. Presently global sea surface topography is inferred from multi-satellite altimeters combination (Jason-2, Criosat-2, Altika), being able to resolve features of about 50 km at weekly time scales [143]. Several projects are now arising to increase the capability of satellite altimetry to resolve even smaller space scales [144], i.e., submesoscales (in the order of 10 km or less), such as the Surface Water and Ocean Topography (SWOT) mission and the Winds and Currents Mission (WaCM). Monitoring and understanding mesoscale and submesoscale dynamics is essential to interpret the variability of many other physical and biological ocean properties [145–148], as well as to investigate the pathways of transport and dispersion of pollutants at sea, such as oil and plastics. Ongoing efforts are currently underway to develop algorithms able to identify oceanic fronts [149, 150], and some active or incoming satellite missions already provide observations that can be used for marine debris monitoring based on sensors originally meant for monitoring other physical and chemical processes at the ocean surface, with promising results (e.g., [49, 50]). Nevertheless, considering the observational limitations of each sensor (related to spectral resolution and range, sensitivity, spatio-temporal resolution, and coverage), the integration of complementary and targeted sensors on the same observing platform represents a significant technological challenge to enhance the performances of marine debris monitoring from space [151]. The combination of concurrent satellite sensors resolving both the physical dynamics (in the near future down to submesoscales) and the distribution and composition of pollutants at the sea surface will provide crucial information on the role of fronts and currents in influencing the transport and dispersion of floating debris.

Remote sensing is also essential in case of oil spill accidents, during which a timely and accurate assessment of the distribution, thickness, and type of the oil patches and slicks is fundamental to plan efficient response and mitigation strategies [152]. Typically, observations of oil spills are provided by visible, infrared, and hyperspectral sensors on board of satellite missions or aerial surveys. Despite the regular availability and global coverage of satellite missions, the identification and

monitoring of a specific spill event can be limited by the time of satellite overpasses and, in case of sensors based on the visible and infrared light spectrum detection, by daylight conditions, cloud cover, or sun glint [153].

Complementary monitoring comes from airborne observations, which can provide targeted surveys of areas affected by oil spills with higher resolution in space and time [154] as well as large-scale surveys of floating macro-litter [155–157]. As for satellite platforms, specific sensors on aircrafts, such as the thermal and imagery components, have also proven their effectiveness in the investigation of small-scale circulation processes with surface signature but related to the dynamics of the upper ocean layer. Rascle et al. [158] and [159] investigated the dynamics of a very intense and sharp (30–50 m) front in the Gulf of Mexico through aerial sun glint images used to retrieve surface roughness and therefore surface current gradients. Their characterization of the frontal activity was confirmed by concurrent remote and in-situ observations, such as satellite SAR and radiometers, X-band radar, and drifters. Another example of airborne observations of the small-scale dynamics is based on infrared images of a very sharp (about 100 m) river plume front surface signature in the Gulf of Mexico (Fig. 3), whose dynamics have been further investigated through in-situ samplings of the water column properties (thermohaline and currents), together with drifter trajectory observations in the proximity of the front [160].

Remote observations of small scale (10–100 m) ocean fronts and of the induced convergence lines trapping floating material can be also retrieved by optically tracking the shape evolution of floater clusters through automated aerial imaging systems mounted on ship-tethered aerostats [161]. In particular, targeted experiments clearly evidenced the influence of sustained wind forcing at the ocean surface, which drives energetic Langmuir circulation. Under such conditions, the floaters dense patch starts aligning in windrows after some minutes from deployment, and in the next hours the windrows spacing grows through windrows merging (Fig. 4). The
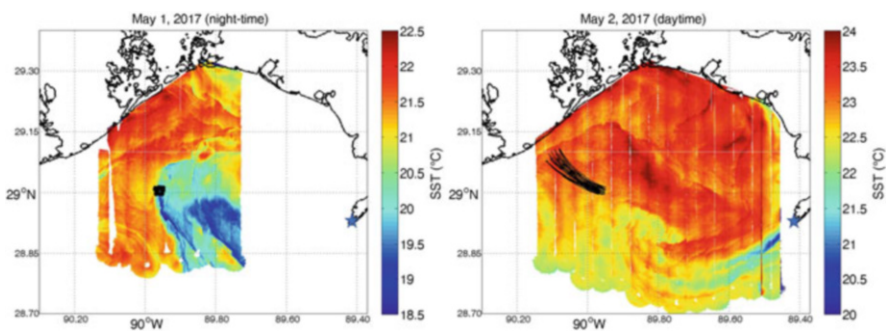

Fig. 3 Left panel: nighttime identification of a plume front (Mississippi river) from airborne infrared images and the contextual deployment of a cluster of drifters along the front (black dots). Right panel: daytime evolution of the same front (advection toward North-West and warm up by sunlight). Black lines represent the trajectories of drifters trapped in the frontal margin. The blue star denotes the position of the river mouth. Color bar limits of the panels are different to enhance details visibility despite daytime temperature excursion (Modified after Solodoch et al. [160])
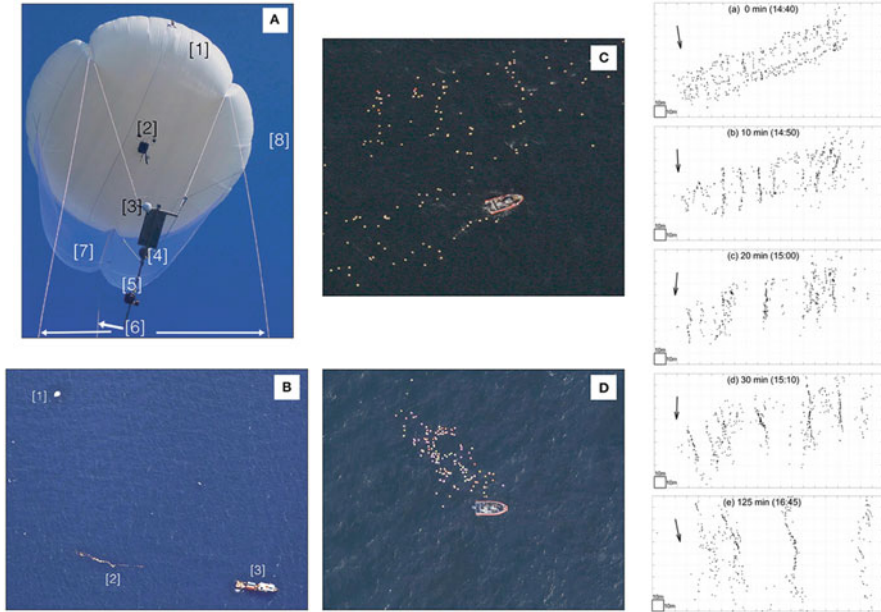
Fig. 4 The study of the formation and evolution over time of Langmuir windrows at the sea surface. Left and middle images (**A–D**): ship-tethered aerostat system with camera providing aerial pictures of bamboo plates cluster deployment and evolution by surface currents. Right panels (**a–e**): rectified plates position and alignment at different times after deployment (Images reproduced from Carlson et al. [161] and Chang et al. [162]. See these papers for a more accurate description of these images)

evolution of the streaks, aligned with the wind, allowed to characterize crosswind and downwind surface dispersion and the spatio-temporal scales involved [162]. These encouraging applications of aerial observations of contaminant dispersion as well as small-scale physical processes further motivate the development of coordinated observations of both aspects; moreover, the use of drones [163] is also very promising to enhance the comprehension of the role of ocean currents in influencing the distribution and transport of plastics and other pollutants at the sea surface [164–166].

5 Large-Scale, Mesoscale, and Submesoscale Frontal Systems: Selected Case Studies

In this section we discuss some specific cases of frontal systems and their potential impact on plastic distribution in the world ocean, going from the large-scale Antarctic Circumpolar Current (ACC), to the mesoscale, describing a NW Mediterranean coastal front, and lastly, to the submesoscale, with a riverine frontal system in

the Northern Gulf of Mexico (GoM). While the scale distinction is very useful to differentiate the main frontal properties, different spatial scales actually interact with each other (as shown in the following sections). Large fronts can be seen as the coalescence of several mesoscale fronts, and mesoscale frontal systems can generate filaments leading to submesoscale fronts and instabilities.

The three case studies differ not only in terms of main scales, but also in terms of basic scientific questions and basic results presented here. The AAC provides a textbook example of how a large-scale frontal system can act as both a barrier and a mixer, because of the great number of processes involved. The nature of the "leakage" through the front and its consequences in terms of transport and tracer distribution is discussed. In the NW Mediterranean case, we concentrate mostly on the specific mechanism of interaction between a mesoscale coastal front and the winds that appear to play a key role in the strengthening and disruption of the front, as well as in the distribution of tracers and plastics. The potential impact of submesoscale features, observed by HF radar within the larger mesoscale frontal system, is also discussed. Finally, in the Northern GoM case, we focus on the influence of submesoscale frontal processes generated by high riverine gradients on the properties of dispersion and trapping of surface tracers. Results from intense in-situ surveys including hundreds of drifters and modeling studies performed in the area during the last decade are discussed, leading to a new perspective on submesoscale frontal dynamics.

5.1 The Antarctic Circumpolar Current: An Imperfect Barrier?

The competition between impermeability and cross-frontal exchange in a jet current has been subject to investigation for decades: a good example of this is provided by studies on the Gulf Stream in this perspective. Back in 1985 Amy Bower and colleagues [167] tried to determine the mutual importance of the two contrasting mechanisms of the current, as "a barrier or a blender," which is still under debate. Different scales of motion appear to play very different roles in such a framework (see, e.g., the very recent paper by [168], who suggest that submesoscale processes may be at the root of an important fraction of the cross-frontal transport). The same ambivalence holds true for one of the most prominent large-scale frontal systems: the Antarctic Circumpolar Current (ACC), where both barring and blending mechanisms seem to coexist. The ACC flows in a latitudinal band of the Southern Ocean dominated by the westerlies, which represent its major forcing. Together with the absence of meridional boundaries (due to emerged land, unique to this latitude range), this zonal pattern of the atmospheric forcing, mediated by the Coriolis effect, allows for the development of a massive circumpolar current connecting the three major ocean basins through the Southern Ocean. This powerful system has in turn a

wide influence on the global ocean circulation, the world's climate and large-scale biogeochemical transport.

As first recognized by Deacon [169], the ACC structure is not that of a simple swift zonal current marking the transition from warm, light subtropical water in the north to cold, dense Antarctic water in the south. The ACC is characterized by a very complex structure of multiple jets and fronts. In their classical definition [170], these fronts develop zonally around the entire Antarctic continent; they are the Southern ACC Front (SACCF), the Polar Front (PF), and the Subantarctic Front (SAF), (see Fig. 5) all encompassed by the Southern Tropical Front, or Northern Boundary (NB) in the North and the so-called Southern Boundary (SB) in the South. They can
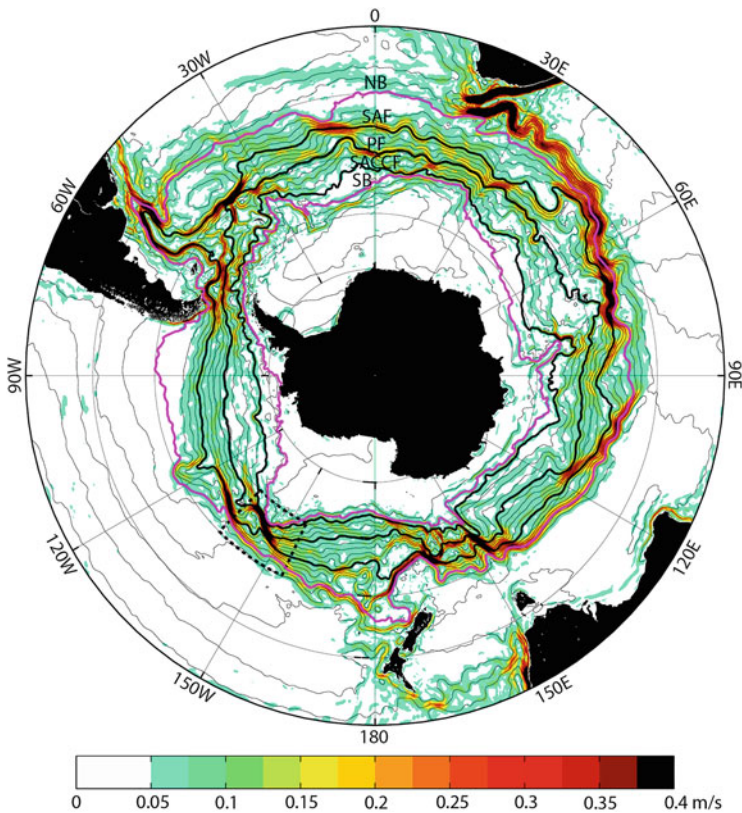

Fig. 5 Mean Dynamic Topography (light black lines every 0.1 m) of the Southern Ocean from the Centre National d'Etudes Spatiales-Collect Localisation Satellites 2018 Mean Dynamic Topography data set. Thick black lines stand for three major Antarctic Circumpolar Current fronts, from the north: SAF = Subantarctic Front; PF = Polar Front; SACCF = Southern Antarctic Circumpolar Current Front. The NB = northern boundary and SB = southern boundary encompassing the Antarctic Circumpolar Current are indicated by thick magenta lines. The color bar refers to the intensity of surface geostrophic currents (Reproduced from Park et al. [171])

be identified in meridional transects as locations of strong property gradients in the horizontal and of steep isopycnal slopes [170].

In the velocity field the latter characteristic is mirrored by maxima of the zonal current [172–174]; this determines the multiple jet pattern which characterizes the ACC. These fronts separate "zones" [175] relatively homogeneous in terms of hydrological and biogeochemical properties and even biological populations, differentiated from, and with little exchange with, one another [173]: the Subantarctic Zone, the Polar Frontal Zone, and the Antarctic Zone [176]. In terms of the three-dimensional velocity field, this is the surface expression of a meridional sequence of convergences and divergences (see the classical association of the Antarctic convergence with the Polar Front by Wyrtky [177]). The barrier effect of such a sharp, banded structure is further enhanced at the surface by the northward Ekman transport associated with the westerlies, in particular in correspondence of the Subantarctic and Polar Fronts [178].

In principle, all the above makes both coastal and offshore Antarctic waters the most isolated region of the global ocean, and for this reason, the Antarctic region has been traditionally considered relatively unaffected by plastic pollution, even though crossing of the Antarctic Polar Front by driftwood and fishing-related materials was already reported in both directions since the early 1960s [179, 180]. In the 1980s, the arrival of microplastics in Antarctic waters was inferred based on the presence of ingested plastics in Antarctic seabird species which remain south of the Polar Front year-round [181, 182], and as a matter of fact, plastic debris has been washing up on sub-Antarctic islands for decades [183–188].

More recently, our view of the circumpolar fronts as impermeable barriers has been further challenged by the evidence that storm-driven surface waves and ocean eddies facilitate crossing of the polar fronts, resulting in more frequent north-south dispersal of drifting kelp and other materials than previously thought [189, 190]. It is thus becoming increasingly clear that circumpolar fronts are not impenetrable, and this finding is further supported by the increasing evidence that the Southern Ocean is not completely exempt from the arrival of plastic pollution from lower latitudes [191–193], suggesting that the Antarctic continent is not as isolated from the rest of the world as previously thought.

The permeability of the ACC occurs most likely where the zonal frontal structure of the current is not sharply defined: splitting and merging of the multiple fronts have been broadly observed in different sectors of the Southern Ocean, giving rise to an intricate structure of the ACC fronts [173, 174, 176, 194–198]. The eddy field has a peculiar importance for the ACC system, because it is key to its response to the atmospheric forcing [172, 199, 200], showing patterns clearly dependent on the bottom topography. In particular, available potential energy due to an increased wind stress yields a growth of available potential energy by increasing the steepness of isopycnals, that is eventually released through baroclinic instability (this is the so-called eddy saturation regime, see [201–203], and references therein). Such instabilities develop mainly in the regions downstream of major topographic features, as nicely illustrated, e.g., by Rintoul [204], which are characterized by meandering motion, where front merging or splitting takes place (Fig. 6).
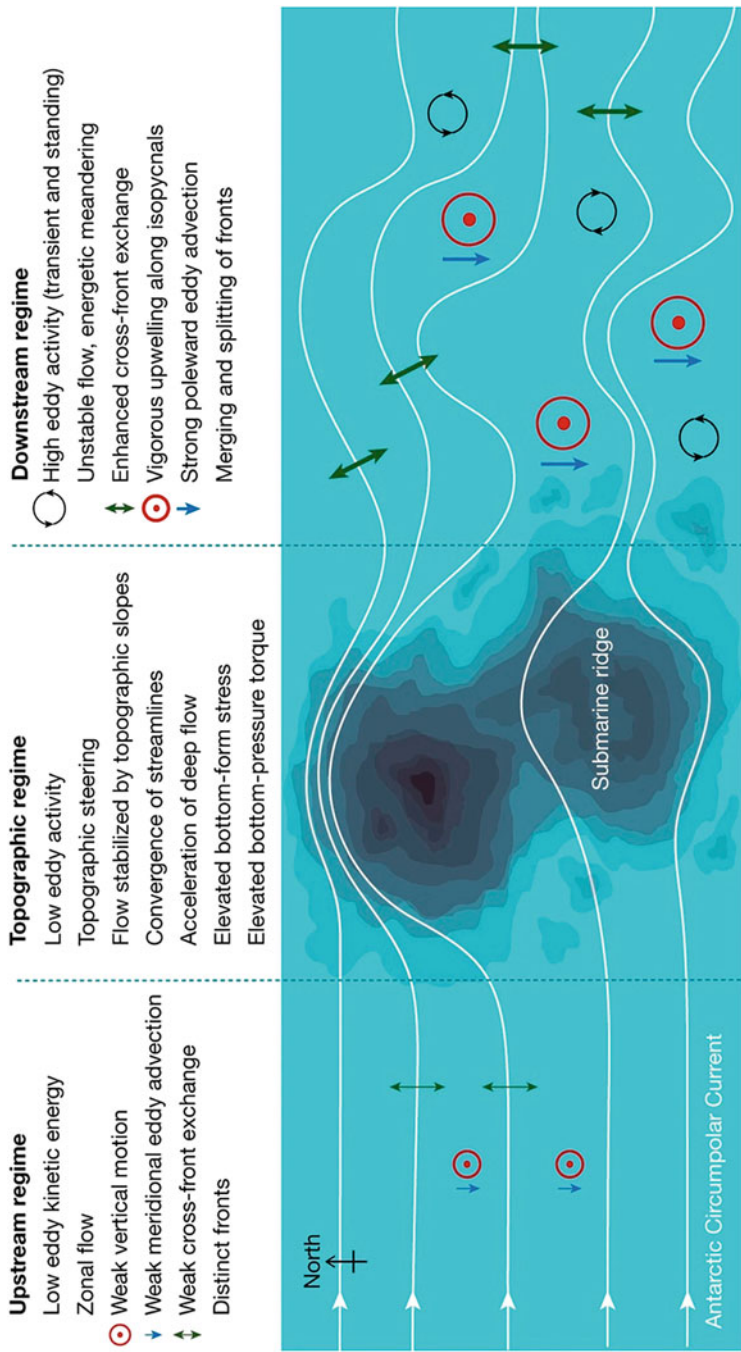
Fig. 6 Processes developing when the ACC interacts with major topographic features (reproduced from Rintoul [204])

What is more important to our context is that these are the regions where enhanced mesoscale eddy activity is responsible for cross-frontal exchange at different depths [205, 206], therefore these instabilities have been defined as "hotspots" of transport, or "leaky jet" segments ([204, 207, 208]; and many references therein).

All the above suggest that the main cross-frontal exchange mechanism, which makes the southernmost portion of the Southern Ocean accessible to floating pollutants, and in particular to plastics, is most likely represented by mesoscale eddy transport. However, the role of these processes in favoring cross-frontal transport of plastics and other buoyant material clearly deserves to be investigated in more detail.

Lastly, it is worth adding that very little is known about submesoscale motions in correspondence of the ACC, stemming from mesoscale features [209, 210]: studies have been mainly focused on their associated vertical transport [211–214], which leaves the question to their possible contribution to cross-frontal transport enhancement open. With this regard, a recent modeling study by Wichmann et al. [215] nicely demonstrated that the role of the ACC in preventing transported matter from entering the Southern Ocean weakens significantly with depth. Moreover, wind- and wave-driven mixing and Langmuir turbulence can greatly enhance the submersion of buoyant plastic debris [216, 217]. Therefore, it can be hypothesized that in the highly dynamic Southern Ocean, microplastics can be more prone to be transported southward by subsurface currents, hence explaining the low concentrations of plastics usually found in Antarctic surface waters [218], especially when compared to subtropical waters north of the STF [192].

As an additional process, Stokes' drift may act as a supplementary cross-frontal, meridional transport mechanism, considering in particular that the Southern Ocean is subject to a very strong wind regime (home to the roaring 40s, furious 50s, and screaming 60s, see https://oceanservice.noaa.gov/facts/roaring-forties.html). Stokes' drift is a second-order effect which causes a weak Lagrangian transport in the direction of propagation of surface waves which is maximal at the surface and decays with depth [219]. Recent modeling studies [190] suggest that the combination of eddy transport and Stokes' drift, in cases of storms, may be at the origin of a limited, occasional meridional "permeability" of the ACC frontal system to biological particle (kelp fragments) southward motion, eventually accessing the periantarctic ocean. As underlined by Onink et al. [24], the incorporation of Stokes drift in Lagrangian simulations can lead to a remarkable increase in the arrival of particles in the Southern Ocean, but it remains unclear whether this is also the case for microplastics and other pollutants, and further investigations on this topic are clearly needed.

5.2 A Mesoscale Front in the NW Mediterranean Sea

The Mediterranean Sea is recognized as one of the world's hot-spot for plastics concentration [6, 11, 156, 220] and in this basin, the concentration of plastics and other pollutants often exceeds by orders of magnitude those reported from the main

Fig. 7 Schematic of the Western Mediterranean circulation: colors represent topography/bathymetry, green arrows show the main circulation branches to the North known as Eastern Corsica Current (ECC), Western Corsica Current (WCC), and Northern Current (NC). The Gulf of Lion (GoL) is an important dense water formation location due to the interaction with Tramontane and Mistral wind (gray arrows). The three boxes show the location of the measurements reviewed in Sect. 5.2 (Modified from Fig. 1 of Berta et al. [77] with permission of the authors)
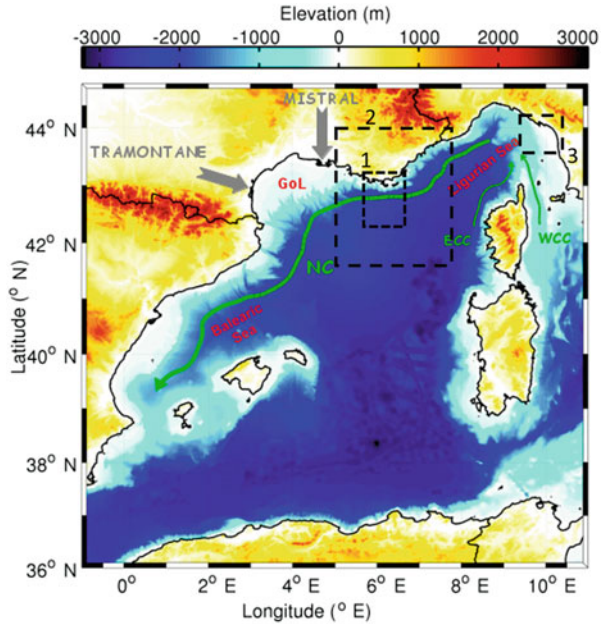
global accumulation zones (i.e., the subtropical gyres). The lack of permanent accumulation zones in the Mediterranean Sea has been already reported by multiple authors [101, 120, 121, 221, 222], and at the same time, a relatively high variability is generally observed in both macro and microplastics distribution surveys [6, 223, 224]. This spatial heterogeneity is likely due to a number of different factors: inhomogeneous distribution of plastic sources, meteorological conditions, sampling designs, methodological considerations, or the effect of surface currents [20, 225, 226]. Although a clear understanding of the respective contribution of all these factors is currently lacking, a better discernment of the spatio-temporal variability in plastic concentrations is important not only because it has obvious implications for the validity of basin-scale estimates, but also because it enables a better targeting of future and ongoing mitigation efforts. In this section, we concentrate on mesoscale processes and their intrinsic variability, by providing some key examples related to a major mesoscale front in the North-Western (NW) Mediterranean Sea.

The NW Mediterranean basin is characterized by a broad cyclonic circulation (Fig. 7) with a well-defined boundary current, the Northern Current (NC), or Liguro-Provencal current. The NC is characterized by a frontal zone, separating lighter coastal waters of Atlantic origin [227, 228] from the denser interior water masses, and it has been intensively studied in the last decades from both the experimental and modeling points of view. It forms from the confluence of two northward branches flowing on both sides of the Corsica Island and flows westward in the upper 200–300 m along the continental slope of Italy, France, and Spain. It is strongly seasonally modulated [229–232], with an extended width of approximately 40 km and relatively weak flow (<50 cm/s) during summer, while during winter the flow
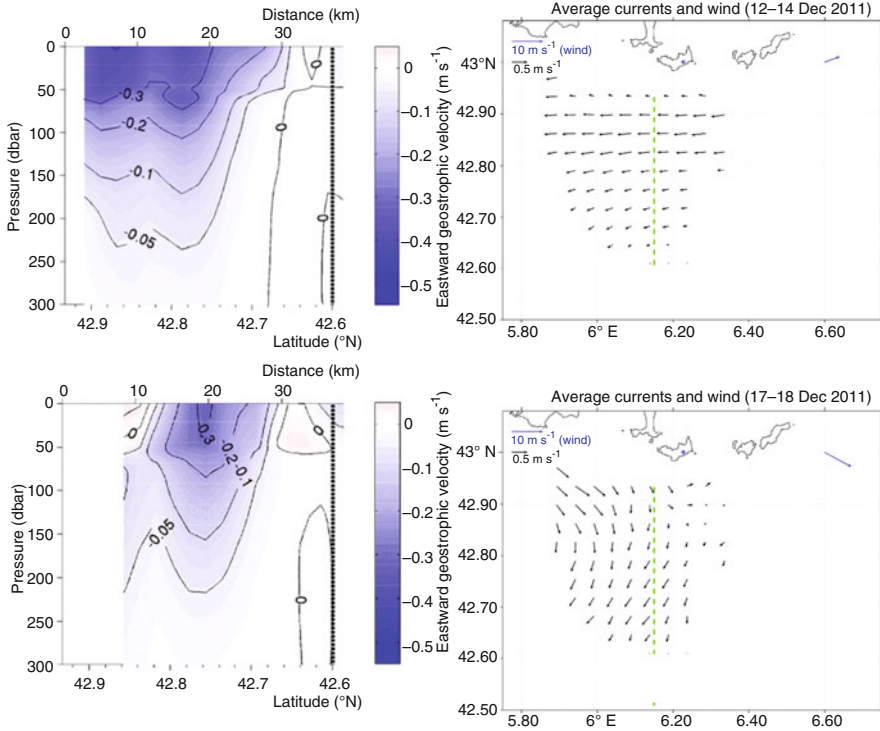
Fig. 8 Examples of Northern Current velocity measured by HF radar (right panels) and glider (left panels) during a calm wind period (upper panels), and a period dominated by westerly winds (lower panels). The black arrows in the right panels are the surface currents from HFR averaged during the period in which the glider transect (green dashed line) falls inside the HFR coverage (Box 1 of Fig. 7). The left panels show the geostrophic velocity along the transect as computed from the hydrographic glider data (modified from Figs. 5 and 6 of Berta et al. [77] with permission of the authors)

accelerates up to 100 cm/s, moves closer to the coast becoming narrower and deeper and the transport increases up to 2 Sv. The flow is also strongly modulated by meso and submesoscale instabilities [227, 233], especially during winter, as well as by meteorological forcing responses [74, 234].

From the dynamical point of view, the NC is a mesoscale current delimited by a frontal area which is primarily characterized by geostrophic balance. Figure 8 (upper right panel) shows a typical velocity pattern at the sea surface, characterized by an along-slope maximum, as measured by HF radars in the area of Toulon in a period of calm winds in December (see Box 1 in Fig. 7). The corresponding depth-dependent geostrophic velocity within the frontal region is shown in Fig. 8 (upper left panel) as estimated by hydrographic data collected along a glider section. The interesting point is that the surface values of the geostrophic velocity exactly coincide with the values measured by HF radars along the section [77], confirming the predominant geostrophic nature of the current. Such balance, though, can be strongly altered by

the presence of instabilities and even more so by meteorological forcing. An example is shown in Fig. 8 (lower panels), in presence of a westerly wind lasting more than 3 days, that causes upwelling in the water column, disrupting the front and causing offshore surface transport as captured by the radar. Indeed, in this case the geostrophic velocity strongly differs from the surface radar velocity and the interior current transport decreases to approximately half of its values reaching 0.5 Sv.

As shown in Fig. 8, wind effects play a fundamental role in inducing ageostrophic processes in the frontal NC. Prevailing winds in the area are along the same axis as the current, but they can be either in the same direction as the current (easterlies) or opposite to it (westerlies). Westerly winds, blowing opposite to the current direction, cause upwelling and tend to move offshore the current core. When they are sufficiently strong and long lasting, the NC front can actually be temporarily disrupted and arrested. Easterly winds, on the other hand, blow in the same direction as the current and are downwelling prone and tend to sharpen the front and move the core of the current toward the coast [234].

Modifications to the frontal zone and processes of frontogenesis and frontolysis can also occur because of dynamical instabilities of the system. Mesoscale instabilities in the NC are prevalent [227, 235] and are characterized by the formation of meanders and the generation of secondary circulation with vertical velocities close to the front, as diagnosed in the framework of quasi-geostrophic dynamics [236]. Enhanced vertical motion is expected to occur in presence of submesoscale processes when the geostrophic balance breaks [39, 70], especially within frontal boundaries and filaments. Indications of submesoscale instabilities in the NC are shown also by glider sections [237]. Even though vertical velocities have not been directly measured in the NC front, interior physical and biological patterns suggest that vertical processes are likely to be very relevant [228, 238–240].

Overall, the processes summarized above suggest that the NC frontal zone can impact the distribution and transport of tracers, and in particular of plastics, in several ways:

1. The basic structure of the mesoscale frontal zone and associated currents are expected to induce enhanced horizontal shear dispersion within the current, while acting as a barrier toward the rest of the basin.
2. The barrier effect is expected to be disrupted in presence of flow instabilities and even more so in case of strong winds. Westerly winds are expected to move surface plastics offshore, while easterly winds can generate an onshore stranding effect.
3. Instabilities and wind forcing in the frontal zone can lead to frontogenetic effects, and induce accumulation of buoyant materials at the front. Vertical velocities, with expected subduction from the dense side of the front can influence the vertical distribution of microplastics in a way that depends on their properties and distribution.

Observations of smaller microplastics in the NW Mediterranean area [221, 241, 242], on the other hand, do not show accumulation patterns in the frontal zone. It is not clear at this point whether this is due to the sparse sampling that does not allow to

Fig. 9 Floating marine litter distribution observed along the French Riviera (Box 2, Fig. 7) during the EcoOcean cruises (October 2006–October 2008) superimposed to the mean surface velocity. Large and small circles mark the positions and dates of observed high (>10 items/km^2) and low (<10 items/km^2) concentrations of floating debris, respectively (Reproduced from Ourmières et al. [243])
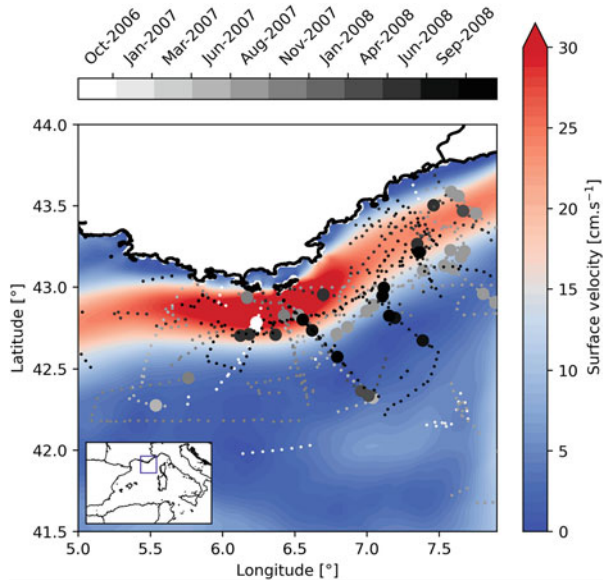
effectively resolve the front, or whether indeed the response of microplastics is different from the response of buoyant macroplastics. This could be due to the complex interplay between the physical processes, including vertical cells, and the nature and sources of microplastics, its buoyancy as a function of materials and fragmentation history. Further studies are needed to sort these points out.

Direct measurements of plastics in the NC frontal zone are scarce, but a first synthesis of results obtained from repeated surveys of floating marine debris has been provided by Ourmières et al. [243] in the French Riviera (Box 2 in Fig. 7). Visual surveys of floating litter were performed as part of the Marine Strategy Framework Directive along 67 transects in the period 2006–2008 [244, 245]. The results are summarized in Fig. 9 where measured floating litter concentrations are shown, superimposed to the NC path as depicted from a numerical model in terms of surface velocity field averaged over the transects period [243]. In most surveys, higher debris concentrations were reported in the NC core and frontal zone, despite the potential importance of coastal sources. Only in 18% of the cases, high litter concentrations were observed offshore with respect to the front, and in most of these cases, a westerly upwelling prone wind event occurred in the previous weeks. From repeated beach survey observations of stranded litter carried out in three beaches in 2010, episodic enhancement appears to be connected not only to rainfall effects on the local river, but also to the occurrence of easterly, downwelling prone winds, in agreement also with previous observations of jellyfish stranding on beaches [234]. Overall, these results are in good agreement with what can be expected from the frontal dynamics effects summarized above.

Another interesting aspect that should be further investigated by future research is the potential role of submesoscale features and coastal eddies on plastic distribution.
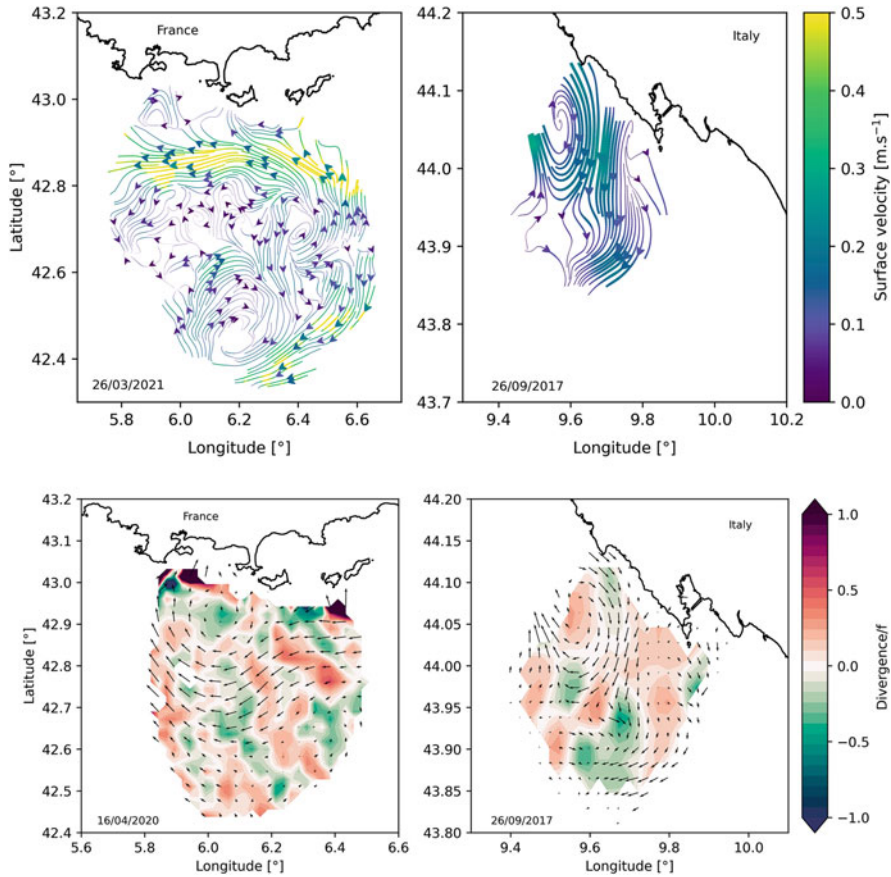
Fig. 10 HF radar surface currents measured on the 26th of April 2021 in the area of Toulon, France (left panels, corresponding to Box 1 of Fig. 7), and in the area of La Spezia, Italy (right panels, corresponding to Box 3 of Fig. 7) measured on the 26th of September 2017. Vorticity/f (upper) and Divergence/f (lower panels) colored background are superimposed to the velocity field

While the NC has a well-defined structure (as shown in Fig. 8), in most areas where the continental shelf is narrow, there are other areas along its path where the presence of an extended shelf allows for the formation of submesoscale vortices, especially during the summer period when the current is weaker. This is the case, for instance, in the Eastern Ligurian Sea (Box 3 in Fig. 7) and in the area of Toulon (Box 1 Fig. 7) as evidenced by HF radar observations. Figure 10, shows an example of small-scale features (order of 5–7 km) depicted from HF radar at both locations at different dates. These features are characterized by high values of divergence and vorticity reaching order f (Coriolis parameter; Berta et al. [246]). As shown by Goldstein et al. [20] and Gove et al. [32], the presence of submesoscale features with high divergence values can lead to a high spatio-temporal inhomogeneity in plastic concentration, with this having obvious implications when trying to extrapolate general features in plastic distribution based on sparse microplastic samples and discrete macro-litter observations.

5.3   Submesoscale Fronts in the Northern Gulf of Mexico

The Gulf of Mexico (GoM) is highly affected by anthropic activities with several consequences, going from frequent red tides episodes [247], massive oil spills due to platform failures or explosions [248], and high macro- and microplastic concentrations [249, 250]. The large-scale circulation in the GoM is dominated by the Loop Current (LC) entering from the Yucatan Channel and flowing anti-cyclonically eastward, while occasionally shedding large LC eddies and displaying a wide variety of oscillations [251]. In the Northern GoM, the circulation is due to an interplay between occasional eddy intrusion, wind forcing, and the outflow of the Mississippi River, entering the Gulf through the typical bird foot delta. The river influx causes a web of freshwater filaments, creating extended regions characterized by submesoscale fronts with extensive submesoscale instabilities [252]. The Deepwater Horizon (DwH) oil spill occurred in the Northern Gulf in 2010 and it is considered to be the largest marine oil spill in the history of the petroleum industry. This event was a dramatic demonstration of the effects of such circulation on transport, since oil is a good tracer and millions of barrels of oil were released into the ocean for almost 3 months, making the impact of convergence regions on the distribution of surface material visibly evident compared to many past oceanographic experiments. However, images taken during this disaster did not provide adequate scientific quantification of the effect of fronts on ocean surface transport.

With the objective of understanding processes that may influence transport of oil near the surface of the ocean, as well as evaluating the accuracy of current-generation ocean models, the CARTHE Consortium (http://carthe.org/) carried out several field campaigns in the northern Gulf of Mexico in the last few years. Due to the high information content and high spatio-temporal variability of ocean fronts, a large number of biodegradable drifters [89] were selected as the observation main tool (Fig. 2). In addition to GPS drifters, a variety of new instruments were created for this program to achieve unprecedented levels of dense and overlapping datasets that span a wide range of spatial and temporal scales (Fig. 11). The reader is referred to Lund et al. [114], Carlson et al. [161], Chang et al. [162], and Lodise et al. [253] for a detailed description of the results obtained from the spectrum of tools shown in Fig. 11.

Overall, on the basis of Gulf of Mexico experiments, the influence of oceanic fronts on the transport of flotsam can be summarized as follows:

1. *Modified dispersion*: On the basis of two-point dispersion metrics, data from 300 drifters released during the Grand LAgrangian Deployment (GLAD) clearly show local or scale dependent transport across all scales measured (summarized in [252] and references therein). A dispersion deficit in the submesoscale/convergent regime can occur when these processes are not resolved adequately in ocean general circulation models. This local dispersion hypothesis contrasts with the alternative hypothesis being that mesoscales can govern dispersion at all scales, including smaller ones (see Fig. 2 in [254]). Once the dispersion rates are measured, it is possible to parameterize this Lagrangian drift in ocean models,
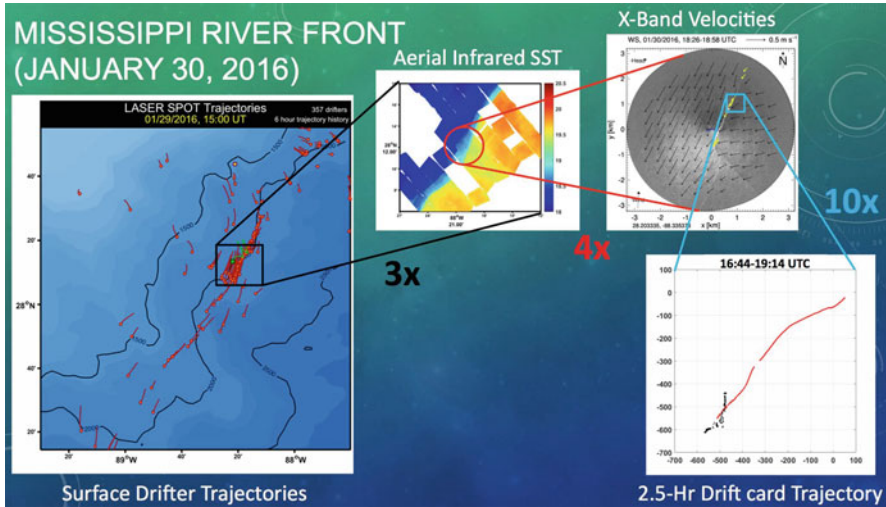
Fig. 11 Collection of overlapping observations from an experiment performed in the Gulf of Mexico, in which different instruments were used to progressively zoom in by a factor of 120x (Image courtesy of Dr. Henry Chang). The reader is referred to Lund et al. [114], Carlson et al. [161], Chang et al. [162], and Lodise et al. [253] for a detailed description of the results obtained from the spectrum of tools shown here

using Lagrangian subgrid models presented in Haza et al. [255]. Poje et al. [252] also showed that geostrophic currents derived from altimeters have large differences, further strengthening the point that ageostrophic (submesoscale) processes are responsible for this difference. By using an ocean model as well as real drifters' trajectories, Pearson et al. [256] showed that over scales <10 km, second-order structure functions of surface drifters consistently have shallower slopes than Eulerian statistics, suggesting that surface drifter structure functions differ systematically. The main reason for this discrepancy is the anisotropy when drifters encounter fronts at scales below 10 km. As shown in a modeling study by Haza et al. [257], enhanced dispersion by submesoscales is not limited to northern Gulf of Mexico where freshwater fronts are in abundance. Mixed layer instabilities taking place along the rim of mesoscale eddies can also create enhanced dispersion by facilitating the flotsam to leak through the mesoscale transport barriers.

2. *Trapping and blocking of surface material*: Huguenard et al. [258], Roth et al. [259], Rascle et al. [158], Androulidakis et al. [260], and Solodoch et al. [160] document that upper ocean fronts created by coastal fresh water outflows act as barriers to transport, exerting a strong influence on the pathways of flotsam coming from the ocean (several examples are shown in Fig. 12). River plume dynamics influence material transport at the surface, its landfall locations and timing. In the coastal experiment described by Solodoch et al. [160] all drifters deployed along the targeted Mississippi plume front that were not recovered by
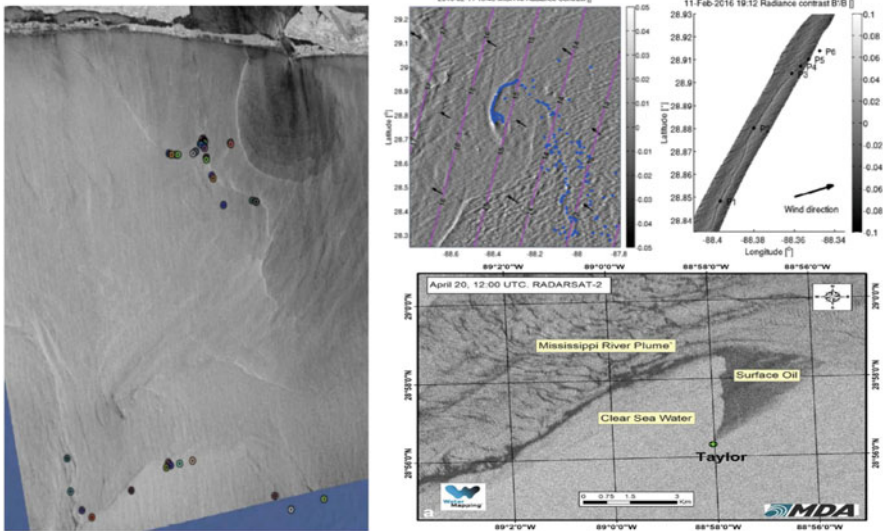
Fig. 12 Images from various expeditions in the Gulf of Mexico showing the impact of upper ocean fronts on blocking the pathways of flotsam. (Left panel) Ocean drifters released in the vicinity of a tidal freshwater outflow near Destin FL during a CARTHE experiment, superimposed on SAR (synthetic aperture radar) image (From Huguenard et al. [258]). (Right upper panels) Drifters (marked in blue and as P1 to P6) released in northern Gulf of Mexico superimposed on airplane-based visible image of sea surface roughness (from Rascle et al. [158]). (Right lower panel) SAR image of Taylor oil spill from northern Gulf of Mexico propagating along the boundary of Mississippi river outflow (from Androulidakis et al. [260]). In all cases, observational data indicate that fronts control transport of upper ocean material

the end of the in-situ survey continued the shoreward propagation and made landfall a few hours later. Trapping of material was known for a long time, but quite dramatic examples of complete blocking and diverting the transport to locations that are hundreds of kilometers from the source of the surface material are documented in the above-mentioned studies. Furthermore, all ocean fronts observed in these Gulf of Mexico experiments had a lateral scale on the $O(1 \text{ m})$, and evolved on time scales of several hours, much smaller and faster than known before.

3. *Vertical transport to depth*: Densely-launched drifter data sets also contain a large number of "ocean sink holes." A very dramatic example is described by D'Asaro et al. [102], where 300 drifters initially deployed by two ships on a frontal region over 30 km by 30 km (the size of a large city) collapsed into 30 m by 30 m (the size of a large classroom), corresponding to a contraction in area by one million times in a few days. Vertical velocities of several cm/s were measured by deploying a Lagrangian float on the dense side of the rolling front. The implication of this observation, made possible only by the availability of large enough number of drifters, is that the creation of cyclonic submesoscale eddies by frontal instabilities (anticyclonic ones are prohibited by inertial instability; Wang and

Özgökmen [261]) causes enough vertical velocity to provide a pathway for material transport from surface to the depth of the oceans (see following section).

6   The Vertical Challenge

There is never enough data in the ocean, and this is particularly true for plastics, which are typically sampled and observed in a non-systematic way, and whose distribution may be highly variable in space and time. However, it has been recognized that what we measure at the ocean surface is a very tiny percentage of the global yearly input of plastics into the ocean (definitely <5%, with estimates as low as 1%, as in Koelmans et al. [262]; but see also Cózar et al. [9] or Kaandorp et al. [263]). These figures have been recently downscaled by Weiss et al. [12], however a substantial fraction of the missing plastic budget is probably found at the bottom of the ocean, even reaching the possible deepest locations [264], part of it is probably trapped in coastal areas [13, 14], ingested by marine biota [265], or fragmented below our current detection limit [266]. Still, another large share of the global plastic budget should be probably sought in the water column [16], that is the largest habitat on Earth, where measurements are challenging, and very scarce.

A (small) number of possible mechanisms have been hypothesized as responsible for plastic sinking in the ocean, such as entrainment into organic and inorganic matter, buoyancy loss due to biofouling, incorporation into fecal pellets or transport through the food web flows [21, 36, 37, 263, 267, 268]. Recent numerical simulations showed that particle properties combined with the global spatio-temporal variability of physical and biological properties can result in different microplastic sinking timescales in different regions of the ocean [29, 269]. Also, flash-flood generated hyperpycnal flows [30] and other extreme events such as tropical cyclones and tsunamis [270–273] have all been suggested to play an important role for the sinking of plastic debris in coastal areas, while much less is known about the offshore sinking processes of the most abundant micrometer-sized particles. We also know that mixing is taking place in the upper ocean when winds blow over the surface with enough energy to activate wave-generated mixing and that microplastics can be advected downwards by these processes. When estimating microplastic densities based upon manta skimming of the upper surface for instance, it has been demonstrated that wind- and wave-driven vertical mixing can noticeably affect the estimation of microplastics concentrations, and correction factors shall be applied to compensate for these subduction mechanisms [216, 217, 274].

In general terms, we expect that plastic sinking is due to several interacting processes, involving both direct gravitational sinking and buoyancy transformation on the one side, and vertical advection by marine currents on the other. Both of these broad mechanisms, and their potential interaction, are today still very far from being satisfactorily understood and the discussion is still open. In a recent paper, Egger et al. [15] suggested that the presence of plastics in the water column is mainly the

result of a direct "fallout" of small plastic fragments from surface waters, based on a positive correlation between the number of plastic debris at the sea surface and the depth-integrated concentrations of plastic fragments in the water column of the Great Pacific Garbage Patch. It should be noted, though, that the sinking mechanisms of marine plastics are still largely unknown, differently from the sinking mechanisms of oil [275], and vertical fluxes of organic matter and other substances that have been relatively well studied. Plastics sedimentation rates greatly depend on the particle size, shape, density, and fouling-mediated drag. Microplastics are an extremely heterogeneous class of solid contaminants, mostly composed by irregularly-shaped fibers and fragments of varying sizes and materials, and experimental research has shown that under steady and dynamic flow conditions, particle shape can noticeably affect microplastic settling rates [276–278].

The possible role of vertical velocities on plastic fluxes is still largely unknown. Being extremely variable in terms of polymer composition and physicochemical characteristics, plastic particles are not the ideal passive tracer, but they can be treated as such at least in first approximation, since many particles, especially those with densities similar to seawater, behave in a comparable way. Identifying 3D transport pathways of passive tracers in the ocean, including the vertical component, is very challenging since vertical velocities are typically orders of magnitude smaller than horizontal velocities, because of the combined effects of stratification and earth rotation. 3D Lagrangian simulations also require a much greater computational efforts if compared to 2D simulations and are thus still limited in number [29, 53, 269, 276, 279]. Yet, there are specific processes that can enhance vertical downward and upward velocities, through the formation of convergent and divergent areas. An important role in this direction is played by the wind. As already discussed in the previous sections, wind induced Ekman transport at large- and mesoscale can cause significant downwelling and upwelling, inducing vertical velocities that can reach, in specific episodes, orders of magnitude of mm/s [53, 280]. Also, at much smaller scales (order 100 m–1 km) the effects of wind and waves at the ocean surface can induce phenomena such as Langmuir cells and windrows with significant vertical velocities capable of causing smaller plastic particles subduction and mixing [51]. This phenomenon is potentially very important because it is ubiquitous in the world ocean, but is expected to be limited to the upper ocean, i.e. the first 10–20 m. This is suggested also by recent results from drifter clusters [281], showing high convergence values at those scales commonly measured at the surface in several areas of the world ocean, while at 15 m depth the values are significantly lower.

Another key element to understand vertical advection is given by frontal dynamics. At the mesoscale, frontal instabilities are expected to generate vertical velocities of the same order as the Ekman induced velocities, i.e. of the order of mm/s [280], acting over significant time and space scales (order of tens of km and weeks). As a matter of fact, Stukel et al. [282] demonstrated that the flux of sinking particles is twice as high at a frontal system, relative to surrounding waters or to non-frontal conditions and that mesoscale fronts may be responsible for over a quarter of total organic carbon sequestration in the California Current. Although the focus of their

work was on organic carbon, it can be assumed that the role of these processes for the global plastic cycle is also likely to be significant.

Frontal dynamics are also intensified and further accelerated at the surface through the formation of submesoscale instabilities [39] that can generate significant vertical velocities, of the order of cm/s [102]. Lapeyre and Klein [283] have shown that thin submesoscale filaments (with a width of 5–10 km) formed by frontogenic eddy interactions are an important source of tracer injection and can lead to large vertical velocities within these structures, concluding that on a global scale, the tracer flux associated with these filaments is as significant as that associated with eddies. Numerical simulations have also shown that buoyant tracers (including microplastics) accumulate at the surface along submesoscale fronts where they are subducted downward into the water column [210].

A possible hypothesis that needs further testing is that submesoscale processes, that are especially prominent in frontal structures, provide a fast and efficient route of transport within the mixed layer until its base (that can be of the order of 50–100 m, depending on ocean region and season), while mesoscale instabilities and associated vertical velocities might be the dominant mechanism to penetrate the deeper ocean on slower but broader scales. This is suggested, for instance, by recent glider observations collected by Mahadevan et al. [75] in a frontal system in the Alboran Sea, showing deep chlorophyll penetration (up to 120–140 m) originated from a mesoscale instability (Fig. 13).

Despite all the progress made in observing and modeling fronts at the surface of the ocean, several knowledge gaps still need to be addressed in order to understand the relevance of submesoscale frontal processes on a global scale. The first is that since submesoscale fronts cover only a small fraction of the ocean's surface, and evolve rapidly, they are hard to find and track using ocean vessels alone. Aerial platforms have limited range and duration, while satellite sensors have spatio-temporal resolution limitations. So, there are clearly observational challenges. Second, the broad probability distributions of these fronts are not known, given the limited observations available. If the frequency deviate from a Gaussian/normal distribution, then this could imply that rare, extreme events, such as the ocean sink hole identified by almost pure coincidence and sheer data density in D'Asaro et al. [102] might in fact govern how plastics and other pollutants are transported into the ocean, similarly to the storm-driven cross-frontal transport observed in the Southern Ocean by Fraser et al. [190].

Finally, just because oceanic fronts are surface signatures of strong vertical downwelling surfaces, this does not mean that they are effective conduits for transporting and sequestering surface material into the ocean's depths. For instance, a Lagrangian float deployed by D'Asaro et al. [102] surfaced later through a broad upwelling zone, without crossing the boundary between the mixed layer base and stratified layers below (Fig. 14). In the case of plastic transport, a possible hypothesis, that would need verification, is that the combination of vertical transport and buoyancy property changes occurring at fronts due to increased biological activity (i.e., fouling) could lead to enhanced and more effective sinking [38]. On the other hand, for neutral or slightly buoyant particles, the death of fouling organism in the
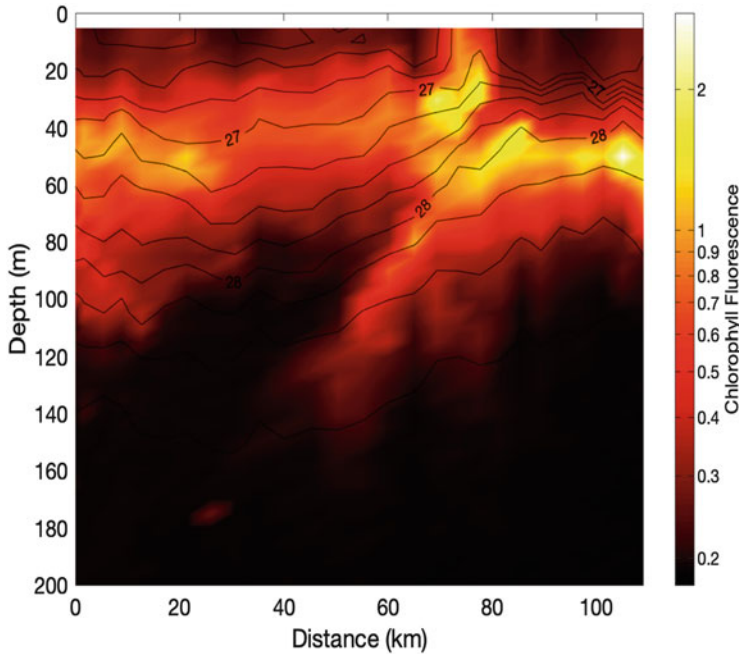
Fig. 13 Chlorophyll (color, log-scale) and density (contours) measured by a glider crossing a gyre front in the Alboran Sea in June 2018, showing the downward advection of phytoplankton from about 50 m to 120 m depth at the front (Reproduced from Fig. 3 of Mahadevan et al. [75] with permission of the authors)

deep would probably lead to a re-surfacing of the particles after a certain amount of time as originally proposed by Ye and Andrady [284], with the so-called yo-yo effect, leading to additional particle redistribution.

Overall, our understanding about the connection between the surface mixed layer, where many plastics and pollutants are first released, and the deeper ocean remains limited, making observation and understanding the vertical transport of material in the ocean a grand challenge. Progress has been made recently in better understanding the so-called Mixed Layer Pump, which appears to contribute significantly to particulate organic carbon export from the mixed layer to the mesopelagic zone especially at high latitudes, where seasonal variations of the mixed layer depth are large [285]. However, whether this process is also relevant for plastic pollution is still unknown. Future research should be aimed at revealing if and how plastic and other contaminants sink at frontal zones, and how relevant these processes are on a global scale, ultimately adding a fundamental piece of knowledge to the plastic puzzle, and helping to finally quantify intercompartmental fluxes between plastic reservoirs (c.f. [286]).
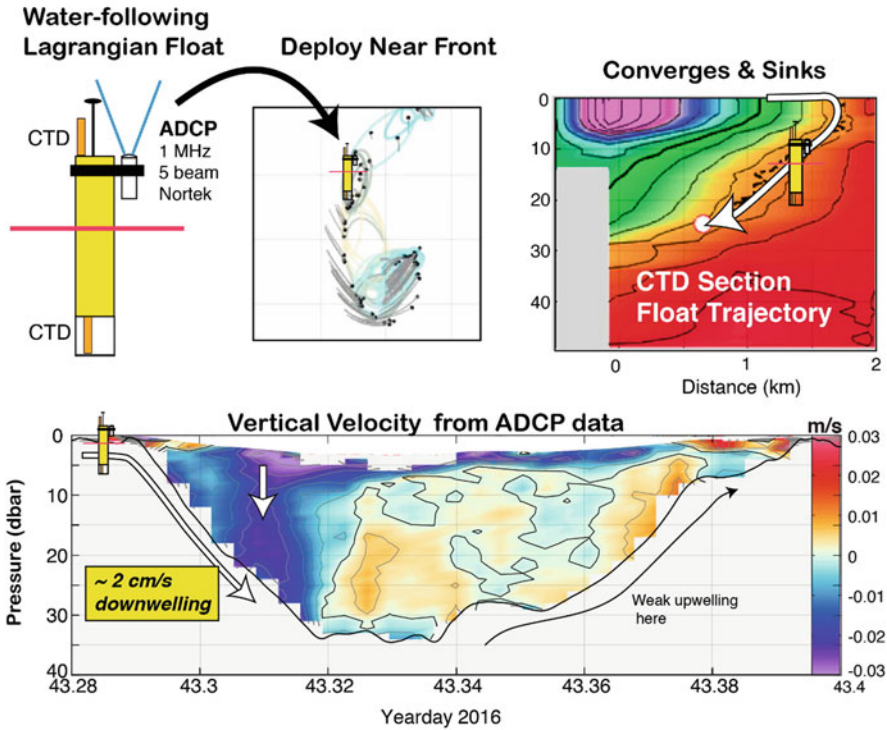
Fig. 14 Behavior of a Lagrangian float deployed along the downwelling frontal boundary of the sink hole as described in D'Asaro et al. [102]

7   Conclusions and Outlook

The global mass of plastic produced by mankind is greater than the overall mass of all terrestrial and marine animals combined [287] and every year, a remarkable portion of mismanaged plastic debris arrives at the ocean surface where it has now become a constant and ubiquitous presence. Nevertheless, our understanding of plastic fluxes, pathways, and fate in oceanic environments is largely incomplete and many of the biological, physical, and geochemical processes that influence the horizontal and vertical transport of plastic at sea (e.g., degradation, sinking, fragmentation, ingestion, beaching) still need to be investigated in detail.

In this chapter we focused our attention on the role of oceanic fronts in influencing the accumulation of plastics and other pollutants, shaping their distribution over the ocean surface, and possibly contributing to their final sinking. We showed that in correspondence with frontal systems, convergence zones potentially accumulate large amounts of floating debris, while at the same time they can favor or prevent the spread of floating material between compartments. We also discussed the still

challenging questions related to the potential role of fronts in the vertical transport of microplastics. Direct measurements of vertical microplastic distribution at fronts are not available yet, and also the investigation of vertical velocity mechanisms is a still open and active area of research, indicating that downwelling frontal areas can potentially export large amounts of debris into the deep sea over relatively short spatio-temporal scales. Oceanic fronts are difficult to locate, but given their ubiquitous presence in the world's ocean, their contribution to the global plastic cycle is probably not negligible and their role in creating surface concentration zones and in removing debris from the sea surface clearly deserves further investigation.

The interaction of mesoscale and submesoscale processes with the general oceanic circulation can potentially create tremendously complex patterns in the distribution of plastic debris. Even an ocean at rest could accommodate a significant inhomogeneity through geographical variation in plastic sources and environmental variables, time-dependent forcings, and different polymer behaviors. Understanding the mechanisms responsible for such a high observed variability in plastic distributions is thus an extremely difficult task. Recent advances in measurement technologies will likely play a pivotal role in advancing future research capabilities. At the same time, the linkage of such measurements with more advanced numerical models (e.g., based on artificial intelligence, data assimilation and machine learning techniques) will likely yield important insights into the mechanisms controlling plastic patchiness in the ocean.

Future research should be focused on better understanding plastic movements in the ocean, in order to more efficiently target intervention and mitigation measures. Being punctiform in space and time, it is becoming increasingly clear that traditional plastic sampling alone is not comprehensive enough to describe complex evolving dynamics such as those involved with frontal systems and oceanic circulation. Improving remote sensing capabilities, developing automated and/or autonomous plastic sensors, and most of all, implementing process-oriented sampling designs are urgent priorities in marine litter research. Estimating the global relevance of all the processes reviewed by this chapter is not an easy task. Future studies should ideally make use of an interdisciplinary array of innovative tools and integrated earth observational instruments that will ultimately enable us to predict and locate more precisely fronts, plastic accumulation areas, concentration hotspots and at last, more effective remediation targets.

References

1. Geyer R, Jambeck JR, Law KL (2017) Production, use, and fate of all plastics ever made. Sci Adv 3:e1700782. https://doi.org/10.1126/sciadv.1700782
2. Lebreton L, Andrady A (2019) Future scenarios of global plastic waste generation and disposal. Palgrave Commun 5:6. https://doi.org/10.1057/s41599-018-0212-7
3. Jambeck JR, Geyer R, Wilcox C et al (2015) Plastic waste inputs from land into the ocean. Science 347:768–771. https://doi.org/10.1126/science.1260352
4. Borrelle SB, Ringma J, Law KL et al (2020) Predicted growth in plastic waste exceeds efforts to mitigate plastic pollution. Science 369:1515–1518. https://doi.org/10.1126/science.aba3656
5. Law KL (2017) Plastics in the marine environment. Annu Rev Mar Sci 9:205–229. https://doi.org/10.1146/annurev-marine-010816-060409
6. Suaria G, Avio CG, Mineo A et al (2016) The Mediterranean plastic soup: synthetic polymers in Mediterranean surface waters. Sci Rep 6:37551. https://doi.org/10.1038/srep37551
7. Tirelli V, Suaria G, Lusher AL (2020) Microplastics in polar samples. In: Rocha-Santos T, Costa M, Mouneyrac C (eds) Handbook of microplastics in the environment. Springer International Publishing, Cham, pp 1–42
8. Gong J, Xie P (2020) Research progress in sources, analytical methods, eco-environmental effects, and control measures of microplastics. Chemosphere 254:126790. https://doi.org/10.1016/j.chemosphere.2020.126790
9. Cozar A, Echevarria F, Gonzalez-Gordillo JI et al (2014) Plastic debris in the open ocean. Proc Natl Acad Sci 111:10239–10244. https://doi.org/10.1073/pnas.1314705111
10. Eriksen M, Lebreton LCM, Carson HS et al (2014) Plastic pollution in the world's oceans: more than 5 trillion plastic pieces weighing over 250,000 tons afloat at sea. PLoS One 9:e111913. https://doi.org/10.1371/journal.pone.0111913
11. van Sebille E, Wilcox C, Lebreton L et al (2015) A global inventory of small floating plastic debris. Environ Res Lett 10:124006. https://doi.org/10.1088/1748-9326/10/12/124006
12. Weiss L, Ludwig W, Heussner S et al (2021) The missing ocean plastic sink: gone with the rivers. Science 373:107–111. https://doi.org/10.1126/science.abe0290
13. Olivelli A, Hardesty BD, Wilcox C (2020) Coastal margins and backshores represent a major sink for marine debris: insights from a continental-scale analysis. Environ Res Lett 15:074037. https://doi.org/10.1088/1748-9326/ab7836
14. Lebreton L, Egger M, Slat B (2019) A global mass budget for positively buoyant macroplastic debris in the ocean. Sci Rep 9:12922. https://doi.org/10.1038/s41598-019-49413-5
15. Egger M, Sulu-Gambari F, Lebreton L (2020) First evidence of plastic fallout from the North Pacific garbage patch. Sci Rep 10:7495. https://doi.org/10.1038/s41598-020-64465-8
16. Pabortsava K, Lampitt RS (2020) High concentrations of plastic hidden beneath the surface of the Atlantic Ocean. Nat Commun 11:4073. https://doi.org/10.1038/s41467-020-17932-9
17. Woodall LC, Sanchez-Vidal A, Canals M et al (2014) The deep sea is a major sink for microplastic debris. R Soc Open Sci 1:140317. https://doi.org/10.1098/rsos.140317
18. Barrett J, Chase Z, Zhang J, Holl MMB, Willis K, Williams A, Hardesty BD, Wilcox C (2020) Microplastic pollution in deep-sea sediments from the Great Australian Bight. Front Mar Sci 7:576170. https://doi.org/10.3389/fmars.2020.576170
19. Thompson RC, Olsen Y, Mitchell RP et al (2004) Lost at sea: where is all the plastic? Science 304:838–838. https://doi.org/10.1126/science.1094559

20. Goldstein MC, Titmus AJ, Ford M (2013) Scales of spatial heterogeneity of plastic marine debris in the Northeast Pacific Ocean. PLoS One 8:e80020. https://doi.org/10.1371/journal.pone.0080020

21. van Sebille E, Aliani S, Law KL et al (2020) The physical oceanography of the transport of floating marine debris. Environ Res Lett 15:023003. https://doi.org/10.1088/1748-9326/ab6d7d

22. Lebreton L, Slat B, Ferrari F et al (2018) Evidence that the great pacific garbage patch is rapidly accumulating plastic. Sci Rep 8:4666. https://doi.org/10.1038/s41598-018-22939-w

23. Brach L, Deixonne P, Bernard M-F et al (2018) Anticyclonic eddies increase accumulation of microplastic in the North Atlantic subtropical gyre. Mar Pollut Bull 126:191–196. https://doi.org/10.1016/j.marpolbul.2017.10.077

24. Onink V, Wichmann D, Delandmeter P, Sebille E (2019) The role of Ekman currents, geostrophy, and stokes drift in the accumulation of floating microplastic. J Geophys Res Oceans 124:1474–1490. https://doi.org/10.1029/2018JC014547

25. Shanks AL (1987) The onshore transport of an oil spill by internal waves. Science 235:1198–1200. https://doi.org/10.1126/science.235.4793.1198

26. Stanev EV, Ricker M (2019) The fate of marine litter in semi-enclosed seas: a case study of the Black Sea. Front Mar Sci 6:660. https://doi.org/10.3389/fmars.2019.00660

27. Zhang Z, Wang W, Qiu B (2014) Oceanic mass transport by mesoscale eddies. Science 345:322–324. https://doi.org/10.1126/science.1252418

28. Canals M, Pham CK, Bergmann M et al (2020) The quest for seafloor macrolitter: a critical review of background knowledge, current methods and future prospects. Environ Res Lett. https://doi.org/10.1088/1748-9326/abc6d4

29. Lobelle D, Kooi M, Koelmans AA et al (2021) Global modeled sinking characteristics of biofouled microplastic. J Geophys Res Oceans. https://doi.org/10.1029/2020JC017098

30. Pierdomenico M, Casalbore D, Chiocci FL (2019) Massive benthic litter funnelled to deep sea by flash-flood generated hyperpycnal flows. Sci Rep 9:5330. https://doi.org/10.1038/s41598-019-41816-8

31. Gardner WD, Richardson MJ, Mishonov AV (2018) Global assessment of benthic nepheloid layers and linkage with Upper Ocean dynamics. Earth Planet Sci Lett 482:126–134. https://doi.org/10.1016/j.epsl.2017.11.008

32. Gove JM, Whitney JL, McManus MA et al (2019) Prey-size plastics are invading larval fish nurseries. PNAS 116:24143–24149. https://doi.org/10.1073/pnas.1907496116

33. González Carman V, Acha EM, Maxwell SM et al (2014) Young green turtles, Chelonia mydas, exposed to plastic in a frontal area of the SW Atlantic. Mar Pollut Bull 78:56–62. https://doi.org/10.1016/j.marpolbul.2013.11.012

34. Josse E, Dagorn L, Bertrand A (2000) Typology and behaviour of tuna aggregations around fish aggregating devices from acoustic surveys in French Polynesia. Aquat Living Resour 13:183–192. https://doi.org/10.1016/S0990-7440(00)00051-6

35. Fazey FMC, Ryan PG (2016) Biofouling on buoyant marine plastics: an experimental study into the effect of size on surface longevity. Environ Pollut 210:354–360. https://doi.org/10.1016/j.envpol.2016.01.026

36. Kooi M, van Nes EH, Scheffer M, Koelmans AA (2017) Ups and downs in the ocean: effects of biofouling on vertical transport of microplastics. Environ Sci Technol 51:7963–7971. https://doi.org/10.1021/acs.est.6b04702

37. Kowalski N, Reichardt AM, Waniek JJ (2016) Sinking rates of microplastics and potential implications of their alteration by physical, biological, and chemical factors. Mar Pollut Bull 109:310–319. https://doi.org/10.1016/j.marpolbul.2016.05.064

38. Kaiser D, Kowalski N, Waniek JJ (2017) Effects of biofouling on the sinking behavior of microplastics. Environ Res Lett 12:124003. https://doi.org/10.1088/1748-9326/aa8e8b

39. McWilliams JC (2021) Oceanic frontogenesis. Annu Rev Mar Sci 13:227–253. https://doi.org/10.1146/annurev-marine-032320-120725

40. Lapeyre G, Klein P, Hua BL (2006) Oceanic restratification forced by surface frontogenesis. J Phys Oceanogr 36:1577–1590. https://doi.org/10.1175/JPO2923.1
41. Acha EM, Piola A, Iribarne O, Mianzan H (2015) Ecological processes at marine fronts: oases in the ocean. Springer, Cham
42. Belkin IM, Cornillon PC, Sherman K (2009) Fronts in large marine ecosystems. Prog Oceanogr 81:223–236. https://doi.org/10.1016/j.pocean.2009.04.015
43. Mann KH, Lazier JRN (2006) Dynamics of marine ecosystems: biological-physical interactions in the oceans.3rd edn. Blackwell Pub, Malden
44. Klemas V, Polis DF (1977) A study of density fronts and their effects on coastal pollutants. Remote Sens Environ 6:95–126. https://doi.org/10.1016/0034-4257(77)90009-8
45. Klemas V (1980) Remote sensing of coastal fronts and their effects on oil dispersion. Int J Remote Sens 1:11–28. https://doi.org/10.1080/01431168008948208
46. Spall MA (1995) Frontogenesis, subduction, and cross-front exchange at upper ocean fronts. J Geophys Res 100:2543. https://doi.org/10.1029/94JC02860
47. Arias M, Sumerot R, Delaney J et al (2021) Mapping windrows as proxies for marine litter monitoring from space (WASP). EGU general assembly 2021, online, 19–30 Apr 2021, EGU21-15275. https://doi.org/10.5194/egusphere-egu21-15275
48. Martínez-Vicente V, Clark JR, Corradi P et al (2019) Measuring marine plastic debris from space: initial assessment of observation requirements. Remote Sens 11:2443. https://doi.org/10.3390/rs11202443
49. Topouzelis K, Papageorgiou D, Suaria G, Aliani S (2021) Floating marine litter detection algorithms and techniques using optical remote sensing data: a review. Mar Pollut Bull 170:112675. https://doi.org/10.1016/j.marpolbul.2021.112675
50. Biermann L, Clewley D, Martinez-Vicente V et al (2020) Finding plastic patches in coastal waters using optical satellite data. Sci Rep 10:5364. https://doi.org/10.1038/s41598-020-62298-z
51. Cózar A, Aliani S, Basurko OC et al (2021) Marine litter windrows: a strategic target to understand and manage the ocean plastic pollution. Front Mar Sci 8:571796. https://doi.org/10.3389/fmars.2021.571796
52. Gutow L, Ricker M, Holstein JM et al (2018) Distribution and trajectories of floating and benthic marine macrolitter in the south-eastern North Sea. Mar Pollut Bull 131:763–772. https://doi.org/10.1016/j.marpolbul.2018.05.003
53. Ricker M, Stanev EV (2020) Circulation of the European northwest shelf: a Lagrangian perspective. Ocean Sci 16:637–655. https://doi.org/10.5194/os-16-637-2020
54. Ruiz I, Basurko OC, Rubio A et al (2020) Litter windrows in the south-east coast of the Bay of Biscay: an ocean process enabling effective active fishing for litter. Front Mar Sci 7:308. https://doi.org/10.3389/fmars.2020.00308
55. Shanks AL (2021) Observational evidence and open questions on the role of internal tidal waves on the concentration and transport of floating plastic debris. Front Mar Sci 8:621062. https://doi.org/10.3389/fmars.2021.621062
56. Liu K, Courtene-Jones W, Wang X et al (2020) Elucidating the vertical transport of microplastics in the water column: a review of sampling methodologies and distributions. Water Res 186:116403. https://doi.org/10.1016/j.watres.2020.116403
57. Mensa JA, Garraffo Z, Griffa A et al (2013) Seasonality of the submesoscale dynamics in the Gulf Stream region. Ocean Dyn 63:923–941. https://doi.org/10.1007/s10236-013-0633-1
58. McWilliams JC (2019) A survey of submesoscale currents. Geosci Lett 6:3. https://doi.org/10.1186/s40562-019-0133-3
59. The MODE Group (1978) The mid-ocean dynamics experiment. Deep-Sea Res 25:859–910. https://doi.org/10.1016/0146-6291(78)90632-X
60. Holland W (1978) The role of mesoscale eddies in the general circulation of the ocean numerical experiments using a wind-driven quasi-geostrophic model. J Phys Oceanogr 8:363–392

61. Fu L, Smith R (1996) Global ocean circulation from satellite altimetry and high-resolution computer simulation. Bull Am Meteorol Soc 77:2625–2636. https://doi.org/10.1175/1520-0477(1996)077%3C2625:GOCFSA%3E2.0.CO;2

62. Ducet N, Le Traon PY, Reverdin G (2000) Global high-resolution mapping of ocean circulation from TOPEX/Poseidon and ERS-1 and -2. J Geophys Res 105:19477–19498. https://doi.org/10.1029/2000JC900063

63. Le Traon PY, Klein P, Hua BL, Dibarboure G (2008) Do altimeter wavenumber spectra agree with the interior or surface quasigeostrophic theory? J Phys Oceanogr 38:1137–1142. https://doi.org/10.1175/2007JPO3806.1

64. Langmuir I (1938) Surface motion of water induced by wind. Science 87:119–123. https://doi.org/10.1126/science.87.2250.119

65. Stanev EV, Ricker M (2020) Interactions between barotropic tides and mesoscale processes in deep ocean and shelf regions. Ocean Dyn 70:713–728. https://doi.org/10.1007/s10236-020-01348-6

66. Tchilibou M, Gourdeau L, Morrow R et al (2018) Spectral signatures of the tropical Pacific dynamics from model and altimetry: a focus on the meso−/submesoscale range. Ocean Sci 14:1283–1301. https://doi.org/10.5194/os-14-1283-2018

67. McWilliams JC (2008) Fluid dynamics at the margin of rotational control. Environ Fluid Mech 8:441–449. https://doi.org/10.1007/s10652-008-9081-8

68. Müller P, McWilliams J, Molemaker M (2005) Routes to dissipation in the ocean: the two-dimensional/three-dimensional turbulence conundrum. In: Baumert HZ, Simpson J, Sündermann J (eds) Marine turbulence: theories, observations, and models. Results of the CARTUM project. Cambridge University Press

69. Munk W, Armi L, Fischer K, Zachariasen F (2000) Spirals on the sea. Proc R Soc Lond A 456:1217–1280. https://doi.org/10.1098/rspa.2000.0560

70. McWilliams JC (2016) Submesoscale currents in the ocean. Proc R Soc A 472:20160117. https://doi.org/10.1098/rspa.2016.0117

71. Klein P, Lapeyre G, Siegelman L et al (2019) Ocean-scale interactions from space. Earth Space Sci 6:795–817. https://doi.org/10.1029/2018EA000492

72. Lévy M, Ferrari R, Franks PJS et al (2012) Bringing physics to life at the submesoscale. Geophys Res Lett 39. https://doi.org/10.1029/2012GL052756

73. Hidalgo-Ruz V, Gutow L, Thompson RC, Thiel M (2012) Microplastics in the marine environment: a review of the methods used for identification and quantification. Environ Sci Technol 46:3060–3075. https://doi.org/10.1021/es2031505

74. Mai L, Bao L-J, Shi L et al (2018) A review of methods for measuring microplastics in aquatic environments. Environ Sci Pollut Res 25:11319–11332. https://doi.org/10.1007/s11356-018-1692-0

75. Mahadevan A, Pascual A, Rudnick DL et al (2020) Coherent pathways for vertical transport from the surface ocean to interior. Bull Am Meteorol Soc 101:E1996–E2004. https://doi.org/10.1175/BAMS-D-19-0305.1

76. Thomas LN, Tandon A, Mahadevan A (2008) Submesoscale processes and dynamics. In: Hecht MW, Hasumi H (eds) Geophysical monograph series. American Geophysical Union, Washington, pp 17–38

77. Berta M, Bellomo L, Griffa A et al (2018) Wind-induced variability in the northern current (northwestern Mediterranean Sea) as depicted by a multi-platform observing system. Ocean Sci 14:689–710. https://doi.org/10.5194/os-14-689-2018

78. Manso-Narvarte I, Fredj E, Jordà G et al (2020) 3D reconstruction of ocean velocity from high-frequency radar and acoustic Doppler current profiler: a model-based assessment study. Ocean Sci 16:575–591. https://doi.org/10.5194/os-16-575-2020

79. Manso-Narvarte I, Rubio A, Jordà G et al (2021) Three-dimensional characterization of a coastal mode-water eddy from multiplatform observations and a data reconstruction method. Remote Sens 13:674. https://doi.org/10.3390/rs13040674

80. Chiba S, Saito H, Fletcher R et al (2018) Human footprint in the abyss: 30 year records of deep-sea plastic debris. Mar Policy 96:204–212. https://doi.org/10.1016/j.marpol.2018.03.022

81. Choy CA, Robison BH, Gagne TO et al (2019) The vertical distribution and biological transport of marine microplastics across the epipelagic and mesopelagic water column. Sci Rep 9:7843. https://doi.org/10.1038/s41598-019-44117-2

82. Boufadel M, Liu R, Zhao L et al (2020) Transport of oil droplets in the upper ocean: impact of the eddy diffusivity. J Geophys Res Oceans 125. https://doi.org/10.1029/2019JC015727

83. Fabregat Tomàs A, Poje AC, Özgökmen TM, Dewar WK (2016) Dynamics of multiphase turbulent plumes with hybrid buoyancy sources in stratified environments. Phys Fluids 28:095109. https://doi.org/10.1063/1.4963313

84. Soloviev AV, Haus BK, McGauley MG et al (2016) Surface dynamics of crude and weathered oil in the presence of dispersants: laboratory experiment and numerical simulation. J Geophys Res Oceans 121:3502–3516. https://doi.org/10.1002/2015JC011533

85. Röhrs J, Dagestad K-F, Asbjørnsen H et al (2018) The effect of vertical mixing on the horizontal drift of oil spills. Ocean Sci 14:1581–1601. https://doi.org/10.5194/os-14-1581-2018

86. Davis RE (1985) Drifter observations of coastal surface currents during CODE: the method and descriptive view. J Geophys Res 90:4741. https://doi.org/10.1029/JC090iC03p04741

87. Niiler PP, Sybrandy AS, Bi K et al (1995) Measurements of the water-following capability of holey-sock and TRISTAR drifters. Deep-Sea Res I Oceanogr Res Pap 42:1951–1964. https://doi.org/10.1016/0967-0637(95)00076-3

88. Centurioni LR, Turton J, Lumpkin R et al (2019) Global in situ observations of essential climate and ocean variables at the air–sea interface. Front Mar Sci 6:419. https://doi.org/10.3389/fmars.2019.00419

89. Novelli G, Guigand CM, Cousin C et al (2017) A biodegradable surface drifter for ocean sampling on a massive scale. J Atmos Ocean Technol 34:2509–2532. https://doi.org/10.1175/JTECH-D-17-0055.1

90. D'Asaro EA, Carlson DF, Chamecki M et al (2020) Advances in observing and understanding small-scale open ocean circulation during the Gulf of Mexico research initiative era. Front Mar Sci 7:349. https://doi.org/10.3389/fmars.2020.00349

91. van Sebille E, Griffies SM, Abernathey R et al (2018) Lagrangian Ocean analysis: fundamentals and practices. Ocean Model 121:49–75. https://doi.org/10.1016/j.ocemod.2017.11.008

92. Alberto F, Raimondi PT, Reed DC et al (2011) Isolation by oceanographic distance explains genetic structure for Macrocystis pyrifera in the Santa Barbara Channel. Mol Ecol 20:2543–2554. https://doi.org/10.1111/j.1365-294X.2011.05117.x

93. Berline L, Rammou A-M, Doglioli A et al (2014) A connectivity-based eco-regionalization method of the Mediterranean Sea. PLoS One 9:e111978. https://doi.org/10.1371/journal.pone.0111978

94. Carlson DF, Griffa A, Zambianchi E et al (2016) Observed and modeled surface Lagrangian transport between coastal regions in the Adriatic Sea with implications for marine protected areas. Cont Shelf Res 118:23–48. https://doi.org/10.1016/j.csr.2016.02.012

95. White C, Selkoe KA, Watson J et al (2010) Ocean currents help explain population genetic structure. Proc R Soc B 277:1685–1694. https://doi.org/10.1098/rspb.2009.2214

96. Sciascia R, Berta M, Carlson DF et al (2018) Linking sardine recruitment in coastal areas to ocean currents using surface drifters and HF radar: a case study in the Gulf of Manfredonia, Adriatic Sea. In situ observations/current field/surface/Mediterranean Sea. Ocean Sci 14 (6):1461–1482

97. Celentano P, Falco P, Zambianchi E (2020) Surface connection between the Ionian Sea and different areas of the Mediterranean derived from drifter data. Deep-Sea Res I Oceanogr Res Pap 166:103431. https://doi.org/10.1016/j.dsr.2020.103431

98. Jönsson BF, Watson JR (2016) The timescales of global surface-ocean connectivity. Nat Commun 7:11239. https://doi.org/10.1038/ncomms11239

99. Maximenko N, Hafner J, Niiler P (2012) Pathways of marine debris derived from trajectories of Lagrangian drifters. Mar Pollut Bull 65:51–62. https://doi.org/10.1016/j.marpolbul.2011.04.016

100. van Sebille E, England MH, Froyland G (2012) Origin, dynamics and evolution of ocean garbage patches from observed surface drifters. Environ Res Lett 7:044040. https://doi.org/10.1088/1748-9326/7/4/044040

101. Zambianchi E, Trani M, Falco P (2017) Lagrangian transport of marine litter in the Mediterranean Sea. Front Environ Sci 5. https://doi.org/10.3389/fenvs.2017.00005

102. D'Asaro EA, Shcherbina AY, Klymak JM et al (2018) Ocean convergence and the dispersion of flotsam. PNAS 115:1162–1167. https://doi.org/10.1073/pnas.1718453115

103. Meyerjürgens J, Badewien TH, Garaba SP et al (2019) A state-of-the-art compact surface drifter reveals pathways of floating marine litter in the German bight. Front Mar Sci 6:58. https://doi.org/10.3389/fmars.2019.00058

104. Schöneich-Argent RI, Freund H (2020) Trashing our own "backyard" – investigating dispersal and accumulation of floating litter from coastal, riverine, and offshore sources in the German Bight using a citizen science-based wooden drifter recapture approach. Mar Environ Res 162:105115. https://doi.org/10.1016/j.marenvres.2020.105115

105. Taylor GI (1922) Diffusion by continuous movements. Proc Lond Math Soc s2-20:196–212. https://doi.org/10.1112/plms/s2-20.1.196

106. Ottino JM (1989) The kinematics of mixing: stretching, chaos, and transport. Cambridge University Press, Cambridge

107. LaCasce JH (2008) Statistics from Lagrangian observations. Prog Oceanogr 77:1–29. https://doi.org/10.1016/j.pocean.2008.02.002

108. Corrado R, Lacorata G, Palatella L et al (2017) General characteristics of relative dispersion in the ocean. Sci Rep 7:46291. https://doi.org/10.1038/srep46291

109. Jacobs GA, D'Addezio JM, Bartels B, Spence PL (2021) Constrained scales in ocean forecasting. Adv Space Res 68:746–761. https://doi.org/10.1016/j.asr.2019.09.018

110. Lebreton LC-M, Greer SD, Borrero JC (2012) Numerical modelling of floating debris in the world's oceans. Mar Pollut Bull 64:653–661. https://doi.org/10.1016/j.marpolbul.2011.10.027

111. Paduan JD, Washburn L (2013) High-frequency radar observations of ocean surface currents. Annu Rev Mar Sci 5:115–136. https://doi.org/10.1146/annurev-marine-121211-172315

112. Roarty H, Cook T, Hazard L et al (2019) The global high frequency radar network. Front Mar Sci 6:164. https://doi.org/10.3389/fmars.2019.00164

113. Rubio A, Mader J, Corgnati L et al (2017) HF radar activity in European coastal seas: next steps toward a pan-European HF radar network. Front Mar Sci 4. https://doi.org/10.3389/fmars.2017.00008

114. Lund B, Haus BK, Horstmann J et al (2018) Near-surface current mapping by shipboard marine X-band radar: a validation. J Atmos Ocean Technol 35:1077–1090. https://doi.org/10.1175/JTECH-D-17-0154.1

115. Serafino F, Bianco A (2021) Use of X-band radars to monitor small garbage islands. Remote Sens 13:3558. https://doi.org/10.3390/rs13183558

116. Holt J, Umlauf L (2008) Modelling the tidal mixing fronts and seasonal stratification of the northwest European continental shelf. Cont Shelf Res 28:887–903. https://doi.org/10.1016/j.csr.2008.01.012

117. Mahadevan A (2006) Modeling vertical motion at ocean fronts: are nonhydrostatic effects relevant at submesoscales? Ocean Model 14:222–240. https://doi.org/10.1016/j.ocemod.2006.05.005

118. Martinez E, Maamaatuaiahutapu K, Taillandier V (2009) Floating marine debris surface drift: convergence and accumulation toward the South Pacific subtropical gyre. Mar Pollut Bull 58:1347–1355. https://doi.org/10.1016/j.marpolbul.2009.04.022

119. Carlson DF, Suaria G, Aliani S et al (2017) Combining litter observations with a regional ocean model to identify sources and sinks of floating debris in a semi-Enclosed Basin: the Adriatic Sea. Front Mar Sci 4. https://doi.org/10.3389/fmars.2017.00078

120. Liubartseva S, Coppini G, Lecci R, Clementi E (2018) Tracking plastics in the Mediterranean: 2D Lagrangian model. Mar Pollut Bull 129:151–162. https://doi.org/10.1016/j.marpolbul.2018.02.019

121. Mansui J, Darmon G, Ballerini T et al (2020) Predicting marine litter accumulation patterns in the Mediterranean basin: Spatio-temporal variability and comparison with empirical data. Prog Oceanogr 182:102268. https://doi.org/10.1016/j.pocean.2020.102268

122. Heron M, Prytz A, Kalangi P (1998) Monitoring dispersion of buoyant pollutants using HF ocean surface radar. J Adv Mar Sci Technol Soc 4:231–241

123. Uttieri M, Cianelli D, Nardelli BB et al (2011) Multiplatform observation of the surface circulation in the Gulf of Naples (southern Tyrrhenian Sea). Ocean Dyn 61:779–796. https://doi.org/10.1007/s10236-011-0401-z

124. Mantovanelli A, Heron M (2012) Radar-based tracking of pollutants/larvae in the Coral Sea. In: Proceedings of the 12th international coral reef symposium, Cairns, Australia

125. Bellomo L, Griffa A, Cosoli S et al (2015) Toward an integrated HF radar network in the Mediterranean Sea to improve search and rescue and oil spill response: the TOSCA project experience. J Oper Oceanogr 8:95–107. https://doi.org/10.1080/1755876X.2015.1087184

126. Berta M, Bellomo L, Magaldi MG et al (2014) Estimating Lagrangian transport blending drifters with HF radar data and models: results from the TOSCA experiment in the Ligurian Current (North Western Mediterranean Sea). Prog Oceanogr 128:15–29. https://doi.org/10.1016/j.pocean.2014.08.004

127. Cianelli D, D'Alelio D, Uttieri M et al (2017) Disentangling physical and biological drivers of phytoplankton dynamics in a coastal system. Sci Rep 7:15868. https://doi.org/10.1038/s41598-017-15880-x

128. Boffetta G, Lacorata G, Redaelli G, Vulpiani A (2001) Detecting barriers to transport: a review of different techniques. Phys D Nonlinear Phenom 159:58–70. https://doi.org/10.1016/S0167-2789(01)00330-X

129. Haller G, Yuan G (2000) Lagrangian coherent structures and mixing in two-dimensional turbulence. Phys D Nonlinear Phenom 147:352–370. https://doi.org/10.1016/S0167-2789(00)00142-1

130. Haller G (2015) Lagrangian coherent structures. Annu Rev Fluid Mech 47:137–162. https://doi.org/10.1146/annurev-fluid-010313-141322

131. Nencioli F, d'Ovidio F, Doglioli AM, Petrenko AA (2011) Surface coastal circulation patterns by in-situ detection of Lagrangian coherent structures. Geophys Res Lett 38. https://doi.org/10.1029/2011GL048815

132. Olascoaga MJ, Haller G (2012) Forecasting sudden changes in environmental pollution patterns. Proc Natl Acad Sci 109:4738–4743. https://doi.org/10.1073/pnas.1118574109

133. Haza AC, Özgökmen TM, Griffa A et al (2010) Transport properties in small-scale coastal flows: relative dispersion from VHF radar measurements in the Gulf of La Spezia. Ocean Dyn 60:861–882. https://doi.org/10.1007/s10236-010-0301-7

134. Schroeder K, Chiggiato J, Haza AC et al (2012) Targeted Lagrangian sampling of submesoscale dispersion at a coastal frontal zone: LIDEX10-REP10. Geophys Res Lett 39. https://doi.org/10.1029/2012GL051879

135. d'Ovidio F, Pascual A, Wang J et al (2019) Frontiers in fine-scale in situ studies: opportunities during the SWOT fast sampling phase. Front Mar Sci 6:168. https://doi.org/10.3389/fmars.2019.00168

136. Ghosh A, Suara K, McCue SW et al (2021) Persistency of debris accumulation in tidal estuaries using Lagrangian coherent structures. Sci Total Environ 781:146808. https://doi.org/10.1016/j.scitotenv.2021.146808

137. Suara K, Khanarmuei M, Ghosh A et al (2020) Material and debris transport patterns in Moreton Bay, Australia: the influence of Lagrangian coherent structures. Sci Total Environ 721:137715. https://doi.org/10.1016/j.scitotenv.2020.137715

138. Hernández-Carrasco I, Alou-Font E, Dumont PA, Cabornero A, Allen J, Orfila A (2020) Lagrangian flow effects on phytoplankton abundance and composition along filament-like structures. Prog Oceanogr 189. https://doi.org/10.1016/j.pocean.2020.102469

139. Hernández-Carrasco I, Orfila A, Rossi V et al (2018) Effect of small scale transport processes on phytoplankton distribution in coastal seas. Sci Rep 8:8613. https://doi.org/10.1038/s41598-018-26857-9

140. Fu L-L, Chelton D, Le Traon P-Y, Morrow R (2010) Eddy dynamics from satellite altimetry. Oceanography 23:14–25. https://doi.org/10.5670/oceanog.2010.02

141. Lee T, Hakkinen S, Kelly K et al (2010) Satellite observations of ocean circulation changes associated with climate variability. Oceanography 23:70–81. https://doi.org/10.5670/oceanog.2010.06

142. Lee Z, Shang S, Hu C et al (2010) Time series of bio-optical properties in a subtropical gyre: implications for the evaluation of interannual trends of biogeochemical properties. J Geophys Res 115:C09012. https://doi.org/10.1029/2009JC005865

143. Chelton DB, Schlax MG, Samelson RM (2011) Global observations of nonlinear mesoscale eddies. Prog Oceanogr 91:167–216. https://doi.org/10.1016/j.pocean.2011.01.002

144. Chelton DB, Schlax MG, Samelson RM et al (2019) Prospects for future satellite estimation of small-scale variability of ocean surface velocity and vorticity. Prog Oceanogr 173:256–350. https://doi.org/10.1016/j.pocean.2018.10.012

145. Capet X, McWilliams JC, Molemaker MJ, Shchepetkin AF (2008) Mesoscale to submesoscale transition in the California current system. Part I: flow structure, Eddy flux, and observational tests. J Phys Oceanogr 38:29–43. https://doi.org/10.1175/2007JPO3671.1

146. Klein P, Lapeyre G (2009) The oceanic vertical pump induced by mesoscale and submesoscale turbulence. Annu Rev Mar Sci 1:351–375. https://doi.org/10.1146/annurev.marine.010908.163704

147. Lévy M, Klein P, Treguier A-M (2001) Impact of sub-mesoscale physics on production and subduction of phytoplankton in an oligotrophic regime. J Mar Res 59:535–565. https://doi.org/10.1357/002224001762842181

148. Mahadevan A, Thomas LN, Tandon A (2008) Comment on "Eddy/wind interactions stimulate extraordinary Mid-Ocean plankton blooms". Science 320:448b. https://doi.org/10.1126/science.1152111

149. Li Q, Zhong G, Xie C, Hedjam R (2021) Weak edge identification network for ocean front detection. IEEE Geosci Remote Sens Lett. https://doi.org/10.1109/LGRS.2021.3051203

150. Lima E, Sun X, Yang Y, Dong J (2017) Application of deep convolutional neural networks for ocean front recognition. J Appl Remote Sens 11:1. https://doi.org/10.1117/1.JRS.11.042610

151. Maximenko N, Corradi P, Law KL et al (2019) Toward the integrated marine debris observing system. Front Mar Sci 6:447. https://doi.org/10.3389/fmars.2019.00447

152. Fingas M, Brown C (2017) A review of oil spill remote sensing. Sensors 18:91. https://doi.org/10.3390/s18010091

153. Leifer I, Lehr WJ, Simecek-Beatty D et al (2012) State of the art satellite and airborne marine oil spill remote sensing: application to the BP deepwater horizon oil spill. Remote Sens Environ 124:185–209. https://doi.org/10.1016/j.rse.2012.03.024

154. Zielinski O, Hengstermann T, Robbe N (2006) Detection of oil spills by airborne sensors. In: Gade M, Hühnerfuss H, Korenowski GM (eds) Marine surface films. Springer, Berlin, pp 255–271

155. Garaba SP, Aitken J, Slat B et al (2018) Sensing ocean plastics with an airborne hyperspectral shortwave infrared imager. Environ Sci Technol 52:11699–11707. https://doi.org/10.1021/acs.est.8b02855

156. Lambert C, Authier M, Dorémus G et al (2020) Setting the scene for Mediterranean litterscape management: the first basin-scale quantification and mapping of floating marine debris. Environ Pollut 263:114430. https://doi.org/10.1016/j.envpol.2020.114430

157. Unger B, Herr H, Viquerat S et al (2021) Opportunistically collected data from aerial surveys reveal spatio-temporal distribution patterns of marine debris in German waters. Environ Sci Pollut Res 28:2893–2903. https://doi.org/10.1007/s11356-020-10610-9

158. Rascle N, Molemaker J, Marié L et al (2017) Intense deformation field at oceanic front inferred from directional sea surface roughness observations. Geophys Res Lett 44:5599–5608. https://doi.org/10.1002/2017GL073473

159. Rascle N, Chapron B, Molemaker J et al (2020) Monitoring intense oceanic fronts using sea surface roughness: satellite, airplane, and in situ comparison. J Geophys Res Oceans 125. https://doi.org/10.1029/2019JC015704

160. Solodoch A, Molemaker JM, Srinivasan K et al (2020) Observations of shoaling density current regime changes in internal wave interactions. J Phys Oceanogr 50:1733–1751. https://doi.org/10.1175/JPO-D-19-0176.1

161. Carlson DF, Özgökmen T, Novelli G et al (2018) Surface ocean dispersion observations from the ship-tethered aerostat remote sensing system. Front Mar Sci 5:479. https://doi.org/10.3389/fmars.2018.00479

162. Chang H, Huntley HS, Kirwan AD et al (2019) Small-scale dispersion in the presence of Langmuir circulation. J Phys Oceanogr 49:3069–3085. https://doi.org/10.1175/JPO-D-19-0107.1

163. Johnston DW (2019) Unoccupied aircraft systems in marine science and conservation. Annu Rev Mar Sci 11:439–463. https://doi.org/10.1146/annurev-marine-010318-095323

164. Garcia-Garin O, Borrell A, Aguilar A et al (2020) Floating marine macro-litter in the north western Mediterranean Sea: results from a combined monitoring approach. Mar Pollut Bull 159:111467. https://doi.org/10.1016/j.marpolbul.2020.111467

165. Streßer M, Carrasco R, Horstmann J (2017) Video-based estimation of surface currents using a low-cost quadcopter. IEEE Geosci Remote Sens Lett 14:2027–2031. https://doi.org/10.1109/LGRS.2017.2749120

166. Topouzelis K, Papakonstantinou A, Garaba SP (2019) Detection of floating plastics from satellite and unmanned aerial systems (plastic litter project 2018). Int J Appl Earth Obs Geoinf 79:175–183. https://doi.org/10.1016/j.jag.2019.03.011

167. Bower AS, Rossby HT, Lillibridge JL (1985) The Gulf Stream - barrier or blender? J Phys Oceanogr 15:24–32. https://doi.org/10.1175/1520-0485(1985)015%3C0024:TGSOB%3E2.0.CO;2

168. Wenegrat JO, Thomas LN, Sundermeyer MA et al (2020) Enhanced mixing across the gyre boundary at the Gulf Stream front. Proc Natl Acad Sci U S A 117:17607–17614. https://doi.org/10.1073/pnas.2005558117

169. Deacon G (1937) The hydrology of the Southern Ocean. Discov Rep 15:3–122

170. Orsi AH, Whitworth T, Nowlin WD (1995) On the meridional extent and fronts of the Antarctic circumpolar current. Deep-Sea Res I Oceanogr Res Pap 42:641–673. https://doi.org/10.1016/0967-0637(95)00021-W

171. Park Y-H, Park T, Kim TW, Lee SH, Hong CS, Lee JH, Rio M-H, Pujol MI, Ballarotta M, Durand I, Provost C (2019) Observations of the Antarctic circumpolar current over the Udintsev fracture zone, the narrowest choke point in the Southern Ocean. J Geophys Res Oceans 124(7):4511–4528

172. Falco P, Zambianchi E (2011) Near-surface structure of the Antarctic circumpolar current derived from world ocean circulation experiment drifter data. J Geophys Res 116:C05003. https://doi.org/10.1029/2010JC006349

173. Sokolov S, Rintoul SR (2009) Circumpolar structure and distribution of the Antarctic circumpolar current fronts: 1. Mean circumpolar paths. J Geophys Res 114:C11018. https://doi.org/10.1029/2008JC005108

174. Sokolov S, Rintoul SR (2009) Circumpolar structure and distribution of the Antarctic circumpolar current fronts: 2. Variability and relationship to sea surface height. J Geophys Res 114:C11019. https://doi.org/10.1029/2008JC005248

175. Whitworth T (1980) Zonation and geostrophic flow of the Antarctic circumpolar current at Drake Passage. Deep Sea Res Part A Oceanogr Res Pap 27:497–507. https://doi.org/10.1016/0198-0149(80)90036-9

176. Belkin IM, Gordon AL (1996) Southern Ocean fronts from the Greenwich meridian to Tasmania. J Geophys Res 101:3675–3696. https://doi.org/10.1029/95JC02750

177. Wyrtki K (1960) The Antarctic circumpolar current and the Antarctic polar front. Dtsch Hydrogr Z 13:153–174. https://doi.org/10.1007/BF02226197

178. Talley LD, Pickard GL, Emery WJ (eds) (2011) Descriptive physical oceanography: an introduction.6th edn. Academic Press, Amsterdam

179. Barber HN, Dadswell HE, Ingle HD (1959) Transport of driftwood from South America to Tasmania and Macquarie Island. Nature 184:203–204. https://doi.org/10.1038/184203a0

180. Coombs DS, Landis CA (1966) Pumice from the south sandwich eruption of march 1962 reaches New Zealand. Nature 209:289–290. https://doi.org/10.1038/209289b0

181. Ryan PG (1987) The origin and fate of artefacts stranded on islands in the African sector of the Southern Ocean. Envir Conserv 14:341–346. https://doi.org/10.1017/S0376892900016854

182. van Franeker JA, Bell PJ (1988) Plastic ingestion by petrels breeding in Antarctica. Mar Pollut Bull 19:672–674. https://doi.org/10.1016/0025-326X(88)90388-8

183. Convey P, Barnes D, Morton A (2002) Debris accumulation on oceanic island shores of the Scotia Arc, Antarctica. Polar Biol 25:612–617. https://doi.org/10.1007/s00300-002-0391-x

184. Eriksson C, Burton H, Fitch S et al (2013) Daily accumulation rates of marine debris on sub-Antarctic island beaches. Mar Pollut Bull 66:199–208. https://doi.org/10.1016/j.marpolbul.2012.08.026

185. Gregory M, Kirk R, Mabin M (1984) Pelagic tar, oil, plastics and other litter in surface waters of the NZ sector of the Southern Ocean, and on Ross dependency shores. N Z Antarct Rec 6:12–28

186. Ryan PG (1987) The incidence and characteristics of plastic particles ingested by seabirds. Mar Environ Res 23:175–206. https://doi.org/10.1016/0141-1136(87)90028-6

187. Slip DJ, Burton HR (1991) Accumulation of fishing debris, plastic litter, and other artefacts, on heard and Macquarie Islands in the Southern Ocean. Environ Conserv 18:249–254. https://doi.org/10.1017/S0376892900022177

188. Walker TR, Reid K, Arnould JPY, Croxall JP (1997) Marine debris surveys at Bird Island, South Georgia 1990–1995. Mar Pollut Bull 34:61–65. https://doi.org/10.1016/S0025-326X(96)00053-7

189. Fraser CI, Kay GM, du Plessis M, Ryan PG (2017) Breaking down the barrier: dispersal across the Antarctic polar front. Ecography 40:235–237. https://doi.org/10.1111/ecog.02449

190. Fraser CI, Morrison AK, Hogg AM et al (2018) Antarctica's ecological isolation will be broken by storm-driven dispersal and warming. Nat Clim Change 8:704–708. https://doi.org/10.1038/s41558-018-0209-7

191. Ivar do Sul JA, Barnes DKA, Costa MF et al (2011) Plastics in the Antarctic environment: are we looking only at the tip of the iceberg? Oecol Austr 15:150–170. https://doi.org/10.4257/oeco.2011.1501.11

192. Suaria G, Perold V, Lee JR et al (2020) Floating macro- and microplastics around the Southern Ocean: results from the Antarctic circumnavigation expedition. Environ Int 136:105494. https://doi.org/10.1016/j.envint.2020.105494

193. Waller CL, Griffiths H, Waluda CM et al (2018) Microplastics in the Southern Ocean. Antarct Environ Portal. https://doi.org/10.18124/D4JK8V

194. Anilkumar N, George JV, Chacko R et al (2015) Variability of fronts, fresh water input and chlorophyll in the Indian Ocean sector of the Southern Ocean. N Z J Mar Freshw Res 49:20–40. https://doi.org/10.1080/00288330.2014.924972

195. Billany W, Swart S, Hermes J, Reason CJC (2010) Variability of the Southern Ocean fronts at the Greenwich Meridian. J Mar Syst 82:304–310. https://doi.org/10.1016/j.jmarsys.2010.06.005

196. Kim YS, Orsi AH (2014) On the variability of Antarctic circumpolar current fronts inferred from 1992–2011 altimetry. J Phys Oceanogr 44:3054–3071. https://doi.org/10.1175/JPO-D-13-0217.1

197. Park Y-H, Lee J-H, Durand I, Hong C-S (2014) Validation of Thorpe-scale-derived vertical diffusivities against microstructure measurements in the Kerguelen region. Biogeosciences 11:6927–6937. https://doi.org/10.5194/bg-11-6927-2014

198. Sparrow MD, Heywood KJ, Brown J, Stevens DP (1996) Current structure of the south Indian Ocean. J Geophys Res 101:6377–6391. https://doi.org/10.1029/95JC03750

199. Hughes CW, Ash ER (2001) Eddy forcing of the mean flow in the Southern Ocean. J Geophys Res 106:2713–2722. https://doi.org/10.1029/2000JC900332

200. Morrow R, Coleman R, Church J, Chelton D (1994) Surface eddy momentum flux and velocity variances in the Southern Ocean from Geosat altimetry. J Phys Oceanogr 24:2050–2071. https://doi.org/10.1175/1520-0485(1994)024%3C2050:SEMFAV%3E2.0.CO;2

201. Hogg AMC, Meredith MP, Blundell JR, Wilson C (2008) Eddy heat flux in the Southern Ocean: response to variable wind forcing. J Clim 21:608–620. https://doi.org/10.1175/2007JCLI1925.1

202. Menna M, Cotroneo Y, Falco P et al (2020) Response of the Pacific sector of the Southern Ocean to wind stress variability from 1995 to 2017. J Geophys Res Oceans 125. https://doi.org/10.1029/2019JC015696

203. Thompson AF, Naveira Garabato AC (2014) Equilibration of the Antarctic circumpolar current by standing meanders. J Phys Oceanogr 44:1811–1828. https://doi.org/10.1175/JPO-D-13-0163.1

204. Rintoul SR (2018) The global influence of localized dynamics in the Southern Ocean. Nature 558:209–218. https://doi.org/10.1038/s41586-018-0182-3

205. Naveira Garabato AC, Ferrari R, Polzin KL (2011) Eddy stirring in the Southern Ocean. J Geophys Res 116:C09019. https://doi.org/10.1029/2010JC006818

206. Thompson AF, Sallée J-B (2012) Jets and topography: jet transitions and the impact on transport in the Antarctic circumpolar current. J Phys Oceanogr 42:956–972. https://doi.org/10.1175/JPO-D-11-0135.1

207. Dufour CO, Griffies SM, de Souza GF et al (2015) Role of mesoscale eddies in cross-frontal transport of heat and biogeochemical tracers in the Southern Ocean. J Phys Oceanogr 45:3057–3081. https://doi.org/10.1175/JPO-D-14-0240.1

208. Patel RS, Phillips HE, Strutton PG et al (2019) Meridional heat and salt transport across the subantarctic front by cold-core eddies. J Geophys Res Oceans 124:981–1004. https://doi.org/10.1029/2018JC014655

209. Bachman SD, Taylor JR, Adams KA, Hosegood PJ (2017) Mesoscale and submesoscale effects on mixed layer depth in the Southern Ocean. J Phys Oceanogr 47:2173–2188. https://doi.org/10.1175/JPO-D-17-0034.1

210. Taylor JR (2018) Accumulation and subduction of buoyant material at submesoscale fronts. J Phys Oceanogr 48:1233–1241. https://doi.org/10.1175/JPO-D-17-0269.1

211. Rosso I, Hogg AMC, Kiss AE, Gayen B (2015) Topographic influence on submesoscale dynamics in the Southern Ocean. Geophys Res Lett 42:1139–1147. https://doi.org/10.1002/2014GL062720

212. Rosso I, Hogg AMC, Matear R, Strutton PG (2016) Quantifying the influence of sub-mesoscale dynamics on the supply of iron to Southern Ocean phytoplankton blooms. Deep-Sea Res I Oceanogr Res Pap 115:199–209. https://doi.org/10.1016/j.dsr.2016.06.009

213. Rosso I, Hogg AMC, Strutton PG et al (2014) Vertical transport in the ocean due to sub-mesoscale structures: impacts in the Kerguelen region. Ocean Model 80:10–23. https://doi.org/10.1016/j.ocemod.2014.05.001

214. Siegelman L, Klein P, Rivière P et al (2020) Enhanced upward heat transport at deep submesoscale ocean fronts. Nat Geosci 13:50–55. https://doi.org/10.1038/s41561-019-0489-1

215. Wichmann D, Delandmeter P, van Sebille E (2019) Influence of near-surface currents on the global dispersal of marine microplastic. J Geophys Res Oceans 124:6086–6096. https://doi.org/10.1029/2019JC015328

216. Brunner K, Kukulka T, Proskurowski G, Law KL (2015) Passive buoyant tracers in the ocean surface boundary layer: 2. Observations and simulations of microplastic marine debris. J Geophys Res Oceans 120:7559–7573. https://doi.org/10.1002/2015JC010840

217. Kukulka T, Proskurowski G, Morét-Ferguson S et al (2012) The effect of wind mixing on the vertical distribution of buoyant plastic debris. Geophys Res Lett 39:L07601. https://doi.org/10.1029/2012GL051116

218. Lacerda ALDF, Rodrigues LDS, Van Sebille E et al (2019) Plastics in sea surface waters around the Antarctic peninsula. Sci Rep 9:3977. https://doi.org/10.1038/s41598-019-40311-4

219. Kundu PK (1990) Fluid mechanics. Academic, San Diego

220. Everaert G, De Rijcke M, Lonneville B et al (2020) Risks of floating microplastic in the global ocean. Environ Pollut 267:115499. https://doi.org/10.1016/j.envpol.2020.115499

221. Cózar A, Sanz-Martín M, Martí E et al (2015) Plastic accumulation in the Mediterranean Sea. PLoS One 10:e0121762. https://doi.org/10.1371/journal.pone.0121762

222. Zambianchi E, Iermano I, Suaria G, Aliani S (2014) Marine litter in the Mediterranean Sea: an oceanographic perspective. In: Briand F (ed) Marine litter in the Mediterranean and black seas. CIESM workshop monograph n° 46. CIESM Publisher, Monaco, 180 pp

223. de Haan WP, Sanchez-Vidal A, Canals M (2019) Floating microplastics and aggregate formation in the Western Mediterranean Sea. Mar Pollut Bull 140:523–535. https://doi.org/10.1016/j.marpolbul.2019.01.053

224. Suaria G, Aliani S (2014) Floating debris in the Mediterranean Sea. Mar Pollut Bull 86:494–504. https://doi.org/10.1016/j.marpolbul.2014.06.025

225. Aliani S, Griffa A, Molcard A (2003) Floating debris in the Ligurian Sea, North-Western Mediterranean. Mar Pollut Bull 46:1142–1149. https://doi.org/10.1016/S0025-326X(03)00192-9

226. Aliani S, Molcard A (2003) Hitch-hiking on floating marine debris: macrobenthic species in the Western Mediterranean Sea. Hydrobiologia 503:59–67. https://doi.org/10.1023/B:HYDR.0000008480.95045.26

227. Millot C (1999) Circulation in the western Mediterranean Sea. J Mar Syst 20:423–442. https://doi.org/10.1016/S0924-7963(98)00078-5

228. Stemmann L, Prieur L, Legendre L et al (2008) Effects of frontal processes on marine aggregate dynamics and fluxes: an interannual study in a permanent geostrophic front (NW Mediterranean). J Mar Syst 70:1–20. https://doi.org/10.1016/j.jmarsys.2007.02.014

229. Alberola C, Millot C, Font J (1995) On the seasonal and mesoscale variabilities of the northern current during the PRIMO-0 experiment in the western Mediterranean-Sea. Oceanol Acta 18:163–192

230. Astraldi M, Gasparini GP (1992) The seasonal characteristics of the circulation in the North Mediterranean basin and their relationship with the atmospheric-climatic conditions. J Geophys Res 97:9531. https://doi.org/10.1029/92JC00114

231. Ourmières Y, Zakardjian B, Béranger K, Langlais C (2011) Assessment of a NEMO-based downscaling experiment for the north-western Mediterranean region: impacts on the northern current and comparison with ADCP data and altimetry products. Ocean Model 39:386–404. https://doi.org/10.1016/j.ocemod.2011.06.002

232. Taupier-Letage I, Millot C (1986) General hydrodynamical features in the Ligurian Sea inferred from the dyome experiment. Oceanol Acta 9:119–131

233. Barrier N, Petrenko AA, Ourmières Y (2016) Strong intrusions of the northern Mediterranean current on the eastern Gulf of Lion: insights from in-situ observations and high resolution numerical modelling. Ocean Dyn 66:313–327. https://doi.org/10.1007/s10236-016-0921-7

234. Berline L, Zakardjian B, Molcard A et al (2013) Modeling jellyfish Pelagia noctiluca transport and stranding in the Ligurian Sea. Mar Pollut Bull 70:90–99. https://doi.org/10.1016/j.marpolbul.2013.02.016

235. Sammari C, Millot C, Prieur L (1995) Aspects of the seasonal and mesoscale variabilities of the northern current in the western Mediterranean Sea inferred from the PROLIG-2 and PROS-6 experiments. Deep-Sea Res I Oceanogr Res Pap 42:893–917. https://doi.org/10.1016/0967-0637(95)00031-Z

236. Allen JT, Brown L, Sanders R et al (2005) Diatom carbon export enhanced by silicate upwelling in the northeast Atlantic. Nature 437:728–732. https://doi.org/10.1038/nature03948

237. Niewiadomska K, Claustre H, Prieur L, d'Ortenzio F (2008) Submesoscale physical-biogeochemical coupling across the Ligurian current (northwestern Mediterranean) using a bio-optical glider. Limnol Oceanogr 53:2210–2225. https://doi.org/10.4319/lo.2008.53.5_part_2.2210

238. Boucher J, Ibanez F, Prieur L (1987) Daily and seasonal variations in the spatial distribution of zooplankton populations in relation to the physical structure in the Ligurian Sea Front. J Mar Res 45:133–173. https://doi.org/10.1357/002224087788400891

239. Goffart A, Hecq J, Prieur L (1995) Control of the phytoplankton of the Ligurian Basin by the Liguro-Provencal Front (Corsican sector). Oceanol Acta 18:329–342

240. Sournia A, Brylinski J, Dallot S et al (1990) Fronts hydrologiques au large des côtes françaises : Les sites-ateliers de programme Frontal. Oceanol Acta 13:413–438

241. de Lucia GA, Caliani I, Marra S et al (2014) Amount and distribution of neustonic micro-plastic off the western Sardinian coast (Central-Western Mediterranean Sea). Mar Environ Res 100:10–16. https://doi.org/10.1016/j.marenvres.2014.03.017

242. Pedrotti ML, Petit S, Elineau A et al (2016) Changes in the floating plastic pollution of the Mediterranean Sea in relation to the distance to land. PLoS One 11:e0161581. https://doi.org/10.1371/journal.pone.0161581

243. Ourmières Y, Mansui J, Molcard A et al (2018) The boundary current role on the transport and stranding of floating marine litter: the French Riviera case. Cont Shelf Res 155:11–20. https://doi.org/10.1016/j.csr.2018.01.010

244. Di-Méglio N, Campana I (2017) Floating macro-litter along the Mediterranean French coast: composition, density, distribution and overlap with cetacean range. Mar Pollut Bull 118:155–166. https://doi.org/10.1016/j.marpolbul.2017.02.026

245. Gerigny O, Henry M, Tomasino C, Galgani F (2011) Déchets en mer et sur le fond. in rapport de l'évalution initiale, Plan d'action pour le milieu marin - Mediterranée Occidentale

246. Berta M, Griffa A, Corgnati L et al (2020) Submesoscales variability from surface drifter and HF radar measurements: scale and wind dependence of kinematic properties. In: EGU General Assembly 2020, 4–8 May 2020. EGU2020-18620, Online

247. Sklar FH, Browder JA (1998) Coastal environmental impacts brought about by alterations to freshwater flow in the Gulf of Mexico. Environ Manag 22:547–562. https://doi.org/10.1007/s002679900127

248. Buskey EJ, White HK, Esbaugh AJ (2016) Impact of oil spills on marine life in the Gulf of Mexico: effects on plankton, nekton and deep-sea benthos. Oceanography 29:174–181

249. Di Mauro R, Kupchik MJ, Benfield MC (2017) Abundant plankton-sized microplastic particles in shelf waters of the northern Gulf of Mexico. Environ Pollut 230:798–809. https://doi.org/10.1016/j.envpol.2017.07.030

250. Lecke-Mitchell KM, Mullin K (1992) Distribution and abundance of large floating plastic in the north-central Gulf of Mexico. Mar Pollut Bull 24:598–601. https://doi.org/10.1016/0025-326X(92)90279-F

251. Oey L-Y, Ezer T, Lee H-C (2005) Loop current, rings and related circulation in the Gulf of Mexico: a review of numerical models and future challenges. In: Sturges W, Lugo-Fernandez A (eds) Geophysical monograph series. American Geophysical Union, Washington, pp 31–56

252. Poje AC, Ozgokmen TM, Lipphardt BL et al (2014) Submesoscale dispersion in the vicinity of the deepwater horizon spill. Proc Natl Acad Sci 111:12693–12698. https://doi.org/10.1073/pnas.1402452111

253. Lodise J, Özgökmen T, Gonçalves R et al (2020) Investigating the formation of submesoscale structures along mesoscale fronts and estimating kinematic quantities using Lagrangian drifters. Fluids 5(3):159

254. Özgökmen TM, Poje AC, Fischer PF et al (2012) On multi-scale dispersion under the influence of surface mixed layer instabilities and deep flows. Ocean Model 56:16–30. https://doi.org/10.1016/j.ocemod.2012.07.004

255. Haza AC, Özgökmen TM, Griffa A et al (2012) Parameterization of particle transport at submesoscales in the Gulf Stream region using Lagrangian subgridscale models. Ocean Model 42:31–49. https://doi.org/10.1016/j.ocemod.2011.11.005

256. Pearson J, Fox-Kemper B, Barkan R et al (2019) Impacts of convergence on structure functions from surface drifters in the Gulf of Mexico. J Phys Oceanogr 49:675–690. https://doi.org/10.1175/JPO-D-18-0029.1

257. Haza AC, Özgökmen TM, Hogan P (2016) Impact of submesoscales on surface material distribution in a gulf of Mexico mesoscale eddy. Ocean Model 107:28–47. https://doi.org/10.1016/j.ocemod.2016.10.002

258. Huguenard KD, Bogucki DJ, Ortiz-Suslow DG et al (2016) On the nature of the frontal zone of the Choctawhatchee Bay plume in the Gulf of Mexico. J Geophys Res Oceans 121:1322–1345. https://doi.org/10.1002/2015JC010988

259. Roth MK, MacMahan J, Reniers A et al (2017) Observations of inner shelf cross-shore surface material transport adjacent to a coastal inlet in the northern Gulf of Mexico. Cont Shelf Res 137:142–153. https://doi.org/10.1016/j.csr.2016.12.017

260. Androulidakis Y, Kourafalou V, Özgökmen T et al (2018) Influence of river-induced fronts on hydrocarbon transport: a multiplatform observational study. J Geophys Res Oceans 123:3259–3285. https://doi.org/10.1029/2017JC013514

261. Wang P, Özgökmen TM (2015) How do hydrodynamic instabilities affect 3D transport in geophysical vortices? Ocean Model 87:48–66. https://doi.org/10.1016/j.ocemod.2015.01.002

262. Koelmans AA, Kooi M, Law KL, van Sebille E (2017) All is not lost: deriving a top-down mass budget of plastic at sea. Environ Res Lett 12:114028. https://doi.org/10.1088/1748-9326/aa9500

263. Kaandorp MLA, Dijkstra HA, van Sebille E (2020) Closing the Mediterranean marine floating plastic mass budget: inverse modeling of sources and sinks. Environ Sci Technol 54:11980–11989. https://doi.org/10.1021/acs.est.0c01984

264. Jamieson AJ, Brooks LSR, Reid WDK et al (2019) Microplastics and synthetic particles ingested by deep-sea amphipods in six of the deepest marine ecosystems on earth. R Soc Open Sci 6:180667. https://doi.org/10.1098/rsos.180667

265. López-Martínez S, Morales-Caselles C, Kadar J, Rivas ML (2021) Overview of global status of plastic presence in marine vertebrates. Glob Change Biol 27:728–737. https://doi.org/10.1111/gcb.15416

266. Hale RC, Seeley ME, La Guardia MJ et al (2020) A global perspective on microplastics. J Geophys Res Oceans 125. https://doi.org/10.1029/2018JC014719

267. de la Fuente R, Drótos G, Hernández-García E et al (2021) Sinking microplastics in the water column: simulations in the Mediterranean Sea. Ocean Sci 17:431–453. https://doi.org/10.5194/os-17-431-2021

268. Loughlin C, Marques Mendes AR, Morrison L, Morley A (2021) The role of oceanographic processes and sedimentological settings on the deposition of microplastics in marine sediment: Icelandic waters. Mar Pollut Bull 164:111976. https://doi.org/10.1016/j.marpolbul.2021.111976

269. Mountford AS, Morales Maqueda MA (2019) Eulerian modeling of the three-dimensional distribution of seven popular microplastic types in the global ocean. J Geophys Res Oceans 124:8558–8573. https://doi.org/10.1029/2019JC015050

270. Gündoğdu S, Çevik C, Ayat B et al (2018) How microplastics quantities increase with flood events? An example from Mersin Bay NE Levantine coast of Turkey. Environ Pollut 239:342–350. https://doi.org/10.1016/j.envpol.2018.04.042

271. Lo H-S, Lee Y-K, Po BH-K et al (2020) Impacts of Typhoon Mangkhut in 2018 on the deposition of marine debris and microplastics on beaches in Hong Kong. Sci Total Environ 716:137172. https://doi.org/10.1016/j.scitotenv.2020.137172
272. Murray CC, Maximenko N, Lippiatt S (2018) The influx of marine debris from the Great Japan Tsunami of 2011 to North American shorelines. Mar Pollut Bull 132:26–32. https://doi.org/10.1016/j.marpolbul.2018.01.004
273. Sulistiawati D, Safir M, Putra AE et al (2021) The amount and type of plastics in the Baiya Beach after the Palu Bay tsunami. J Phys Conf Ser 1763:012072. https://doi.org/10.1088/1742-6596/1763/1/012072
274. Kukulka T, Brunner K (2015) Passive buoyant tracers in the ocean surface boundary layer: 1. Influence of equilibrium wind-waves on vertical distributions. J Geophys Res Oceans 120:3837–3858. https://doi.org/10.1002/2014JC010487
275. Jacketti M, Beegle-Krause CJ, Englehardt JD (2020) A review on the sinking mechanisms for oil and successful response technologies. Mar Pollut Bull 160:111626. https://doi.org/10.1016/j.marpolbul.2020.111626
276. Bagaev A, Mizyuk A, Khatmullina L et al (2017) Anthropogenic fibres in the Baltic Sea water column: field data, laboratory and numerical testing of their motion. Sci Total Environ 599–600:560–571. https://doi.org/10.1016/j.scitotenv.2017.04.185
277. Khatmullina L, Isachenko I (2017) Settling velocity of microplastic particles of regular shapes. Mar Pollut Bull 114:871–880. https://doi.org/10.1016/j.marpolbul.2016.11.024
278. Wang Z, Dou M, Ren P, et al (2021) Sedimentation of irregular shaped microplastics under steady and dynamic flow conditions (in Review)
279. Iwasaki S, Isobe A, Kako S et al (2017) Fate of microplastics and mesoplastics carried by surface currents and wind waves: a numerical model approach in the Sea of Japan. Mar Pollut Bull 121:85–96. https://doi.org/10.1016/j.marpolbul.2017.05.057
280. Vélez-Belchí P, Tintoré J (2001) Vertical velocities at an ocean front. Sci Mar 65:291–300. https://doi.org/10.3989/scimar.2001.65s1291
281. Esposito G, Berta M, Centurioni L et al (2021) Submesoscale vorticity and divergence in the Alboran Sea: scale and depth dependence. Front Mar Sci. https://doi.org/10.3389/fmars.2021.678304
282. Stukel MR, Aluwihare LI, Barbeau KA et al (2017) Mesoscale ocean fronts enhance carbon export due to gravitational sinking and subduction. Proc Natl Acad Sci U S A 114:1252–1257. https://doi.org/10.1073/pnas.1609435114
283. Lapeyre G, Klein P (2006) Impact of the small-scale elongated filaments on the oceanic vertical pump. J Mar Res 64:835–851. https://doi.org/10.1357/002224006779698369
284. Ye S, Andrady AL (1991) Fouling of floating plastic debris under Biscayne Bay exposure conditions. Mar Pollut Bull 22:608–613. https://doi.org/10.1016/0025-326X(91)90249-R
285. Lacour L, Briggs N, Claustre H et al (2019) The intraseasonal dynamics of the mixed layer pump in the subpolar North Atlantic Ocean: a biogeochemical-Argo float approach. Global Biogeochem Cycles 33:266–281. https://doi.org/10.1029/2018GB005997
286. Hoellein TJ, Rochman CM (2021) The "plastic cycle": a watershed-scale model of plastic pools and fluxes. Front Ecol Environ. https://doi.org/10.1002/fee.2294
287. Elhacham E, Ben-Uri L, Grozovski J et al (2020) Global human-made mass exceeds all living biomass. Nature 588:442–444. https://doi.org/10.1038/s41586-020-3010-5